ACTA

C

TECHNICA

Mikko Nelo

INKS BASED ON INORGANIC NANOMATERIALS FOR PRINTED ELECTRONICS APPLICATIONS

MIKKO NELO

INKS BASED ON INORGANIC NANOMATERIALS FOR PRINTED ELECTRONICS APPLICATIONS

Academic dissertation to be presented with the assent of the Doctoral Training Committee of Technology and Natural Sciences of the University of Oulu for public defence in the OP auditorium (L10), Linnanmaa, on 4 December 2015, at 12 noon

Nelo, Mikko, Inks based on inorganic nanomaterials for printed electronics applications.
University of Oulu Graduate School; University of Oulu, Faculty of Information Technology and Electrical Engineering, Department of Electrical Engineering
Acta Univ. Oul. C 553, 2015
University of Oulu, P.O. Box 8000, FI-90014 University of Oulu, Finland

Abstract

In this thesis several novel inks based on dry inorganic powders enabling magnetic, piezoelectric and memory resistive (memristive) function were researched for printed electronics applications.

Low curing temperature screen–printable magnetic inks for high frequency applications based on dry cobalt nanoparticles were developed in the first part of the work. Three publications were achieved. The first one concentrated on ink formulation and its process development, the second on the utilization of multifunctional surfactant, and the third on the development of the inks for plastic substrates. The magnetic inks developed were cured at 120 °C. The electrical performance, microstructure, surface quality and mechanical durability of printed and cured layers were investigated. Relative permeability values up to 3 and related loss tangents up to 0.01 were achieved at 2 GHz frequency, as well as a pull–off strength of up to 5.2 MPa. The maximum loading level of cobalt nanoparticles was 60 vol–%, after which the stability of the ink started to degrade. The developed ink enabled the miniaturization of a patch antenna.

In the second part of the thesis, the formulation of inks based on piezoelectric ceramic particles in powder form with ferroelectric polymers as a matrix material is introduced. The performance and quality of the printed inks and cured layers were investigated. The measured pull off –strength was up to 3.25 MPa, relative permittivity was up to 48 at 1 kHz and piezoelectric constant d_{31} up to 17 pm/V. The printed piezoelectric layer can be utilized in a pressure sensor.

In the third part of the thesis, the development of inks for a novel printed memory component, a memristor, is researched. A synthesis route was developed for an organometallic precursor solution, which was formulated into inkjet–printable form. The printing tests were carried out in order to find the most feasible layer thickness with memristive behaviour. The influence of substrate materials and different thermal treatments on the components' electrical properties, durability of read/erase –cycles and overall lifetime were also investigated. The prepared memristive patterns remained functional for up to 35 days, while the precursor solution remained usable for over a year. The memristive areas withstood up to 30 read/erase cycles and by utilizing heat treatments the shift in resistance value increased by up to three orders of magnitude.

Keywords: ink, inkjet printing, magnetic materials, memristor, nanoparticles, piezoelectricity, Printed electronics, screen printing

Nelo, Mikko, Epäorgaanisiin nanomateriaaleihin pohjautuvat musteet painettavan elektroniikan sovelluksiin.
Oulun yliopiston tutkijakoulu; Oulun yliopisto, Tieto- ja sähkötekniikan tiedekunta, Sähkötekniikan osasto
Acta Univ. Oul. C 553, 2015
Oulun yliopisto, PL 8000, 90014 Oulun yliopisto

Tiivistelmä

Väitöstyössä kehitettiin epäorgaanisten kuivien jauhemaisten materiaalien pohjalta magneettisia, pietsosähköisiä ja memristiivisiä musteita käytettäviksi painettavan elektroniikan sovelluksissa.

Työn ensimmäisessä osassa tutkittiin korkean taajuuden sovelluksissa käytettävien magneettisten, matalassa lämpötilassa kovetettavien, jauhemaisiin kobolttinanopartikkeleihin perustuvien silkkipainomusteiden valmistamista. Tulokset on esitetty kolmessa julkaisussa, joista ensimmäinen keskittyi musteen formulointiin, toinen monifunktionaalisen surfaktantin hyödyntämiseen ja kolmas musteen kehittämiseen muovialustalle sopivaksi. Työssä kehitettiin 120 °C:ssa kovettuvia musteita, joista valmistettujen kalvojen suhteellisen permeabiliteetin maksimiarvoksi saatiin 3 ja häviöiden minimiarvoksi 0,01 kahden gigahertsin taajuudella. Pull–off –vetotestin tulokseksi saatiin jopa 5,2 MPa. Musteet säilyivät vakaina enimmillään 60 tilavuusprosentin metallipitoisuudella. Kehitettyä mustetta käytettiin tasoantennin miniatyrisoinnissa.

Toisessa osassa kehitettiin pietsosähköisiä musteita, jotka pohjautuivat keraamijauheeseen ja matriisimateriaalina toimivaan ferrosähköiseen muoviin. Niistä valmistettujen kalvojen parhaaksi pull off –vetotestin tulokseksi saatiin 3,25 MPa, permittiivisyyden maksimiarvoksi 48 yhden kilohertsin taajuudella ja d_{31}–pietsovakion maksimiarvoksi jopa 17 pm/V. Kehitettyjä painettuja rakenteita voidaan käyttää painettavissa paineantureissa.

Kolmannessa osassa kehitettiin uudentyyppinen painettava muistikomponentti, memristori ja komponenttien valmistamiseksi uusi prekursoriliuoksen synteesi. Syntetisoitu liuos muokattiin mustesuihkutulostettavaksi. Painokokeiden avulla selvitettiin materiaalin paksuus, jolla saatiin aikaan muistivastukselle ominainen memristiivinen käyttäytyminen. Työssä tutkittiin substraattimateriaalien ja mahdollisten lämpökäsittelyjen vaikutusta komponenttien sähköisiin ominaisuuksiin, luku/kirjoitussyklien kestoon sekä käyttöikään. Valmistetut memristiiviset kalvot säilyivät toimivina 35 vuorokautta ja prekursoriliuos yli vuoden. Memristiiviset pinnat kestivät jopa 30 luku/kirjoitussykliä ja vastusarvon muutos saatiin lämpökäsittelyllä kolmea kertaluokkaa suuremmaksi.

Asiasanat: magneettiset materiaalit, memristori, musteet, mustesuihkutulostus, nanopartikkelit, Painettava elektroniikka, pietsosähköisyys, silkkipaino

For Katri, Ilona, Olivia and Elena. Love you all.

Acknowledgements

My warmest thanks go to my supervisors, Prof. Heli Jantunen and Docent Jari Juuti for fruitful discussions, support, guidance, patience and encouragement. Having the opportunity to work in this laboratory is the best thing that has happened in my working career. I'm also grateful to Docent Antti Uusimäki for the help and support on scientific writing as well as fruitful discussions on heroic deeds. I want to thank Prof. Tim Button and Dr. Ari Alastalo for the pre–examination of my thesis and for the valuable comments they provided. Prof. Arthur Hill is acknowledged for revising the English language of this thesis and original papers. I am grateful to my co–authors for their hard work on the articles.

There are so many good friends and colleagues in Microelectronics and Materials Physics Laboratories I want to thank for help, advices and good laughs. It has been a privilege and pleasure to work with you. I acknowledge the staff of Center of Microscopy and Nanotechnology for the support and guidance on both on clean room facilities and electron microscopes.

I want to thank all my friends for quality time outside working hours. Sauna evenings, barbecuing, hiking trips and activities involving bicycling are always eagerly awaited. I want to thank my parents Sirpa and Kari for the encouragement for studying during childhood, my sisters Milla and Suvi for friendship and great discussions and my grandmother Raija for all the support. Many thanks for my mother–in law Riitta and sister–in law Mari for giving so good care for our daughters when it was needed.

Most of all, I want to express my deepest love and gratitude to my family: Katri, Ilona, Olivia and Elena. For me, there is nothing more important than you.

List of abbreviations and symbols

BET   Brunauer–Emmett–Teller
DOD   Drop on Demand inkjet
DSC   Differential scanning calorimetry
EDS   Energy–dispersive X–ray spectroscopy
EFTEM   Energy–filtered transmission electron microscopy
FESEM   Field emission scanning electron microscopy
MOD   Metallo–Organic Decomposition ink
MS   Mass spectroscopy
PC   Polycarbonate
PET   Polyethylene terephthalate
PMMA   Poly(methyl methacrylate)
PTF   Polymer Thick Film
PVDF   Poly(Vinylidene Difluoride)
PVDF–TrFE   Poly(Vinylidene Difluoride–Trifluoroethylene)
PZT   Lead Zirconate Titanate
TGA   Thermogravimetric analysis

List of original papers

I   Nelo M, Sowpati AK, Palukuru VK, Juuti J & Jantunen H (2010) Formulation of screen printable cobalt nanoparticle ink for high frequency applications. Progress In Electromagnetics Research 110: 253–266.

II   Nelo M, Sowpati AK, Palukuru VK, Juuti J & Jantunen H (2012) Utilization of screen printed low curing temperature cobalt nanoparticle ink for miniaturization of patch antennas. Progress In Electromagnetics Research 127: 427–444.

III   Nelo M, Myllymäki S, Juuti J, Uusimäki A & Jantunen H (2015) Cobalt nanoparticle inks for printed high frequency applications on polycarbonate. Journal of Electronic Materials 44(12): 4884–4890.

IV   Siponkoski T, Nelo M, Palosaari J, Peräntie J, Sobocinski M, Juuti J & Jantunen H (2015) Electromechanical properties of PZT/P(VDF–TrFE) composite ink printed on a flexible organic substrate. Composites Part B: Engineering 80: 217–222.

V   Nelo M, Sloma M, Kelloniemi J, Puustinen J, Saikkonen T, Juuti J, Häkkinen J, Jakubowska M & Jantunen H (2013) Inkjet–printed memristor – printing process development. Japanese Journal of Applied Physics 52(5): article 05DB21.

In Papers I–III low curing temperature screen printable magnetic inks for high frequency applications were developed on the basis of dry cobalt nanoparticles. The ink formulation process for dry nanoparticles was developed in Paper I. Utilization of multifunctional surfactant and miniaturization of patch antennas were investigated in Paper II, and Paper III presented the development of inks for polycarbonate substrates. The work resulted in multiple inks curing at 120 °C.

In Paper IV piezoelectric inks to be used in, for example, all–printed pressure sensors were developed. Ceramic material in powder form and ferroelectric polymer were used as raw materials, resulting in inks with ceramic content between 30–60 vol.%.

Paper V described the development of a novel printed memory component, a memristor. A new synthesis route for organometallic precursor solutions was developed and further formulated into inkjet–printable form. The influence of electrode materials and different thermal treatments on the components' electrical properties, durability of read/erase –cycles and overall lifetime was investigated.

In papers I–IV the author's contribution was the ink formulations, printing experiments, surface profiler measurements, electron microscopy analyses and mechanical durability measurements. In paper V the author's contribution was the synthesis of the precursor and its formulation to inkjet–printable ink, the printing and post–treatments tests, as well as electron microscopy analyses and planning and guiding of the electrical measurements. Electrical measurements and

component designs carried out in Papers I–IV were done by the co–authors. The x–ray diffraction analysis in Paper V was a contribution of one of the co–authors and in this paper electrical measurements and component designs were done with the second author. All papers were written with the help of the co–authors.

Contents

1   Introduction

1.1   Printed electronics and inks based on inorganic particles

Printed electronics is an increasingly popular method for the production of low–cost or large area consumer electronic devices. The key idea is to use functional printing inks instead of separate components, thus greatly decreasing costs and simplifying the electronics manufacturing processes. The distinctive difference between printed electronics and manufacturing by traditional electronics methods is that printing is additive with an associated low wastage of materials because subtractive processes such as lithography, etching etc. are not needed. This makes printed electronics an interesting option not only for large scale manufacturing but also for making small product batches and prototypes.

The printed components can, for example, be antennas, coils, capacitors, memory components, solar cells or different types of sensors and their integrations. These applications are achieved with combinations of different inks to give the desired properties. Functional materials used in printed electronics can be divided into organic and inorganic groups. Organic materials contain the electrical functionality of the molecules or structures formed by molecules, whereas inorganic materials have their functionality in the crystal structures of the materials. Organic materials are widely researched and utilized in printed electronics in many different fields of application. [1–3]

Possibly the very first conductive ink was patented by Voigt and Haeffner [4] in 1899 describing the invention of "electrical resistance of a thin layer of liquid metal applied by means of firing process". This layer was applied by using a paint consisting of very finely dispersed metal particles and organic compounds. The organic compounds were removed by firing during which the metal particles formed a homogenous metallic layer. Later on in 1945, Deyrup *et al.* [5] produced capacitors based on screen–printed thick films consisting of metal and glass powders fired together. In 1947, thick film based interconnections and passive components were utilized in radio tube modules [6]. The progress of thick film technology rapidly accelerated during the 1960s and 70s when hybrid thick film circuits entered the market. The technology, although requiring high firing temperatures (> 1000 °C), enabled relatively cheap and robust manufacturing methods with trimmability of the passive components, both being advantages

compared to thin film manufacturing methods such as sputtering that requires high vacuum processes. [7]

In recent decades decreasing the processing temperature of inks has been widely researched to enable utilization of flexible substrates like polymers or paper. In particular, Polymer Thick Film (PTF) technology, emerging in the 1980s, provided the possibility of avoiding the firing step completely in certain applications such as resistors. [7]. At the same time PTF consisting of polymer matrices filled with conductive, resistive or dielectric powders was presented to be used for passive component manufacturing by screen printing methods and very low curing temperatures (< 200 °C). Components such as resistors, potentiometers and membrane switches were produced [7, 8]. Basic conductive polymer thick film inks for direct current applications, curing at temperatures suitable for polymer substrates, were introduced in the 1990s [9]. Today, polymeric thick film inks such as graphite inks form one segment of the printed electronics industry, being utilized especially in biosensors.

Very different kinds of inorganic materials in powder form offering applicable electrical properties are typically available at very reasonable prices in large quantities. They are also more stable against oxygen and moisture degradation than are organic materials, which also simplifies the manufacturing of components. Utilizing dry inorganic powders as raw materials for producing low curing temperature printed electronics inks is a rarely used approach. Thus it provides a novel and interesting field of research. The objective of this work was to formulate and produce a variety of functional inks based on inorganic raw materials to be used in printed electronics applications.

1.2   Objective and outline of the thesis

In general, the low temperature curable composite inks are facing several challenges. One of the key issues is the formulation of the ink, enabling its long–term storage as well as uniform dispersion of the filler particles in the desired polymer matrix during curing. In many cases when high electrical performance is expected, also high filler loading levels are needed. However, increasing the loading level of the filler commonly decreases the mechanical durability of the ink and the quality of the printed and cured layers. There are also some applications specific challenges when the composite inks are developed. Especially the layer thickness plays an important role on high frequency or sensor applications requiring careful investigation of feasible binder materials. It is also clear that the

18

printing technique to be used to realize different functional devices must be taken into account when the ink formulations are considered.

The main goal of the thesis is to introduce methods to utilize inorganic materials to provide improved functionality for printed electronics devices through the development of novel low curing temperature inks. The most common way of making functional inks is to synthesize the inorganic material directly into ink, which enables good stabilization of the material [10, 11]. A less researched area is inks that utilize inorganic materials in powder form. This approach is, however, attractive since almost all electrically interesting raw materials are typically available in powder form at a low price. In this thesis, although both approaches were used, the majority of the developed inks were formulated utilizing dry powders. The first chapter describes the background of printed electronics. Chapter 2 describes the most common methods used in printing. Typical ink formulations and analysis methods are also briefly reviewed.

Chapter 3 describes all the materials used in ink formulations in this work, as well as the production and analysis methods used. The ink formulations and characterization of both inks and printed patterns are described on Chapter 4. The first part of this chapter describes the utilization of different surfactants followed by formulation of inks based on magnetic particles. The next part is a description of piezoelectric ink formulations. The synthesis of inks and printing experiments for the memristive components are described at the end of the first half of Chapter 4. The remainder of this chapter describes the analyses carried out on the fabricated components, including surface profiler analysis, electron microscopy analysis of the patterns, adhesion experiments and finally electrical experiments for the memristive layers.

Chapter 5 summarizes the main results of this work, as well as conclusions that were drawn from the research.

2   Printing methods and inks with magnetic, piezoelectric and memristive performance

2.1   Printing methods and demands for inks in flexible electronics

The most feasible printing methods for printed electronics are presented on this chapter. In addition to the printing accuracy (i.e. the smallest feature size and registering accuracy), the layer thickness is also a highly important feature since it plays a significant role in multiple applications such as conductors, capacitors and memory elements.

Table 1 lists some typical properties of the usual printing methods. The highest throughput can be achieved with gravure printing whereas screen printing provides the greatest single layer thickness. If a low layer thickness is desired, inkjet, gravure, flexography and offset printing are the most feasible choices. Although inkjet printing is a slow method, it has by far the best adjustability of the printing pattern during the printing process, making it suitable for fine–tuning the structure to be printed. Especially the gravure, flexography, offset and screen printing methods are suitable for roll–to– roll production, greatly improving the printing speed and suitability for large–scale applications. In roll–to–roll printing, the multiple printing and curing steps are carried out on continuous substrate tape, resulting in the finished printed product at the end of the production line.

Table 1. Parameters of different printing methods. [12, 13].

Printing method	Layer thickness [μm]	Resolution [μm]	Viscosity [mPas]	Throughput [m2/s]
Screen	3 - 100	20 - 100	500-50 000	2 - 3
Inkjet	0.3 - 20	20 - 50	1 - 30	0.01 - 0.05
Gravure	0.8 - 8	75	50 - 200	60
Flexo	0.8 - 2.5	80	50 - 500	10
Offset	0.5 - 2	20 - 50	30 000 - 100 000	5 - 30

2.1.1 Screen printing

Screen printing is a traditional method that is utilized in numerous applications including textiles, advertisements and pottery, but also in electronics. The range of suitable inks is large and the achieved layer thickness is high, giving, for example, good conductivity of printed conductors. A different version of screen printing also

enables printing on flexible or rigid but planar surfaces. On the other hand, the printing speed is not very high (2–3 m^2/s) and the typical achievable resolution is not as high as that of inkjet printing. [14]

In Papers I–III the non–contact screen printing method was used, the operating principle of which is shown in Figure 1. In printing, the ink is pushed with a squeegee through a fine screen. The non–image areas of the screen are covered with emulsion. The print quality is determined by the fineness of the screen, the thickness of the emulsion, the degree of the open area of the screen, the correct viscosity and particle size distribution of the ink. Typically, the ink viscosity is 500– 50 000 mPas and the dried ink film is 3–100 μm thick. [12–15] In Paper IV stencil printing with a doctoring blade was used. In principle this method is very similar to that of contact screen printing, but it enables much thicker layers with a single printing step.
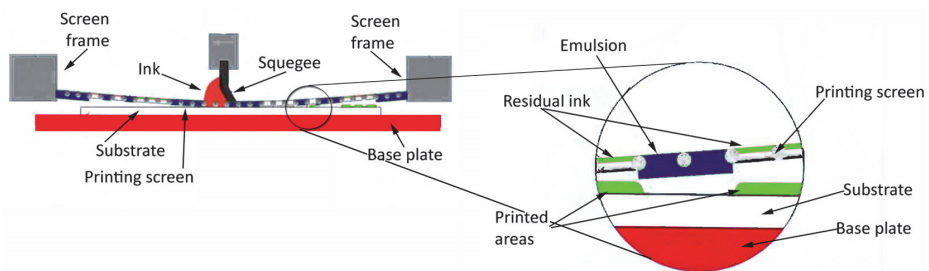
Fig. 1. Principle of screen printing. Redrawn according to H.Kipphan [14].

2.1.2 Inkjet printing

The main benefit of inkjet printing is that it is digital. The pattern to be printed can easily be customized and personalized with only marginal effort via computer control. Inkjet printing is also a non–contact method, which enables printing on both rigid and flexible substrates. Brittle, smooth, rough or even 3D surfaces can be printed. In addition to these benefits, inkjet printing is a precise and high resolution printing tool which consumes only small amounts of printing material. Major drawbacks of this method are low printing speed (0.01–0.05 m^2/s) and printing errors due to nozzle blocking. For some applications such as printed piezoelectric components presented in this work the layer thicknesses achievable with inkjet printing (0.5 – 20 μm, usually less than 5 μm) are too low, making screen printing more suitable option. [12–14]

22

In Paper V a Drop On Demand (DOD) inkjet printer with piezoelectric nozzles (Figure 2) was utilized. In this a piezoelectric crystal generates a pressure pulse that forces an ink drop out of the nozzle orifice. Its benefit is that only acoustic pressure affects the ink during drop formation, enabling the usage of more sensitive materials than with a thermal inkjet printer. [14]
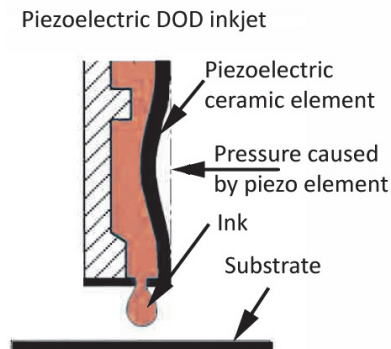
Fig. 2. Principle of DOD inkjet printing. Redrawn according to H.Kipphan [14].

2.1.3 Other printing methods

Gravure printing is typically used for high–quality and high–volume publications and packages. [14]. In gravure printing the printed patterns are engraved into the surface of the printing plate whereas the unpatterned areas remain at the original level. The printing plate is flooded with ink and excess ink is then wiped off with a doctor blade, leaving the ink only in the cells. The ink is then transferred directly onto the substrate in a printing nip under pressure.

The advantages of gravure printing are the simple principle of operation, simply–structured printing equipment, high production speed, high through–put and high resolution. Various solvents can also be used since the printing cylinders are resistant to most solvents and ink chemicals. The disadvantages are expensive printing cylinders (> 1000 €), high demands on substrate surface quality and requirements for precise control of process parameters. The thickness of the ink layer is typically 0.8–2 μm but when UV–curing inks are used the thickness can be up to 8 μm. The ink viscosity is rather low, 50–200 mPas, in order for it to flow easily in and fill out of the engraved cells. [12–14]

Flexography printing has been used mainly in packaging applications. Here, the elements of the printing plate are raised above the base level, forming a relief pattern of the printed image. The printing ink is applied onto the image elements via an anilox roller that has small cells engraved evenly into its surface. The surface of the anilox roller is first flooded with ink from an ink chamber after which excess ink is removed with a doctor blade, leaving ink only in the cells. The ink is then transferred onto the raised image elements of the plate and hence onto the substrate. The plate is made of soft and flexible material (typically photopolymer patterned with UV light) which improves the contact formation at the ink transfer points. The main advantages of flexography printing are a wide variety of suitable substrates, simple operation principle and printer construction, and an accurately adjustable amount of applied ink. Disadvantages include lower print quality, poorer register accuracy and lower printing speed compared to the other contact printing methods. The printed layer thickness is 0.8–1 μm but with UV inks the thickness can be 2.5 μm. The ink viscosity is comparable to that of gravure printing, 50–500 mPas. [12–14, 16–17]

Offset printing is the most common printing method in newspaper and commercial printings in particular when a high print quality is required. It is an indirect printing method where the ink is transferred from the printing plate onto the substrate via an intermediate blanket cylinder. The patterned and unpatterned areas of the plate are on the same level but they have different surface energies: the patterned areas are ink–receptive (hydrophobic) and unpatterned areas ink–repellent but water–accepting (hydrophilic). The plates are typically made of aluminium that is coated with a photopolymer layer. The thickness of the printed film is typically 0.5–1.5 μm. The ink viscosity is very high, 30 000–100 000 mPas, making offset printing an interesting option especially when a very thin and homogeneous printed layer is desired. [12,14]

2.2 Ink formulations

The most common applications of printed electronics today are conductors based on inorganic inks. The inks typically contain metal nanoparticles that are easily sintered into solid conductors with heat [18]. Silver is by far the most popular metal in conductive inks but copper [19], gold [20] and platinum [21] are also used, and research into the use of aluminium [22] has also been carried out. The conductive nanoparticle inks are commonly made by precipitation of metals into suspensions that are further formulated into inks. The metal salt can, for example, be in droplets

24

of surfactant stabilized emulsion, thus obtaining surfactant after the salt has been reduced to metal. The size of the formed nanoparticles can be adjusted by changing the droplet size in the emulsion. [23] Another commonly used method is direct precipitation of particles [24] with the help of stabilizing agents.

Conductive inks can also be made by using solutions of salts of the desired metals and reducing agents for the salts. [25] These types of inks are called Metallo–Organic Decomposition (MOD) inks. During the heat–treatment process, the reducing agent reacts with the metal salt forming solid metal while other reaction products are evaporated. The low metal content of the MOD inks when compared to commercial nanoparticle inks is the main downside. In order to achieve similar layer thicknesses as can be obtained with nanoparticle inks more layers need to be printed.

In addition to conductive inks, there is a vast number of other applications for inorganic inks. They can, for example, be used in capacitor [26] and memory applications [27] and also applications utilizing piezoelectricity such as printed pressure [28] and activity sensors.

2.2.1 Magnetic inks

Magnetic nanoparticles have been traditionally used in various applications such as electromagnetic devices [29], high–density storage media [30,31], ferrofluids [32], magnetic resonant imaging [33], drug delivery [34], and catalysts [35]. Stabilization of cobalt nanoparticle suspensions by the formulation of monolayers of surfactants has been studied [36,37], as well as the formulation of cobalt nanoparticle suspensions by precipitation of cobalt salts into metallic nanoparticles sterically protected by a layer of surfactant [38]. These methods incorporate the synthesis of cobalt nanoparticles during the preparartion of the suspension.

Magnetic metallic cobalt nanoparticles offer an interesting option as a raw material since utilization of solid nanoparticles as a starting point instead of synthesizing them *in situ* would simplify the process substantially. The key issue in this case is to stabilize the dry nanoparticles in a suspension.

2.2.2 Piezoelectric inks

Piezoelectric ceramics, such as lead zirconate titanate (PZT) and polymers are an interesting group of materials that are known for their ability to produce electric potential as a result of the application of pressure, and *vice versa*. They are widely

used as actuators, sensors and transducers in devices from igniters to fine precision printers, sonars and fuel injectors. [39, 40]

A feasible way of making a piezoelectric ink is to formulate a suspension of piezoelectric composite, i.e. a mixture of piezoelectric polymer and ceramic powder. The major challenge in all piezoelectric composites is their low electromechanical performance when compared to that of bulk ceramics or single crystals. However, there are application areas such as sensors where high piezoelectric performance is not necessarily required [41–44].

Poly(vinylidene difluoride) (P(VDF)) and Poly(vinylidene difluoride – trifluoroethylene) P(VDF–TrFE) co–polymers are nowadays well–known options for the polymer matrix of piezoelectric composites. In addition to their potential to form crystalline and piezoelectric structures, they also offer solution–based processibility, low processing temperature and flexibility. [45–52]. P(VDF–TrFE) offers the capability to self–arrange in crystalline form whereas P(VDF) needs stretching in order to achieve an organized crystal structure. This makes P(VDF–TrFE) a good choice for the polymer phase in piezoelectric composite ink.

2.2.3 Memristors

The essential feature of a memristor, i.e. memory resistor, is its hysteretic current–voltage behavior (Figure 3), which enables its use as non–volatile resistive memory.
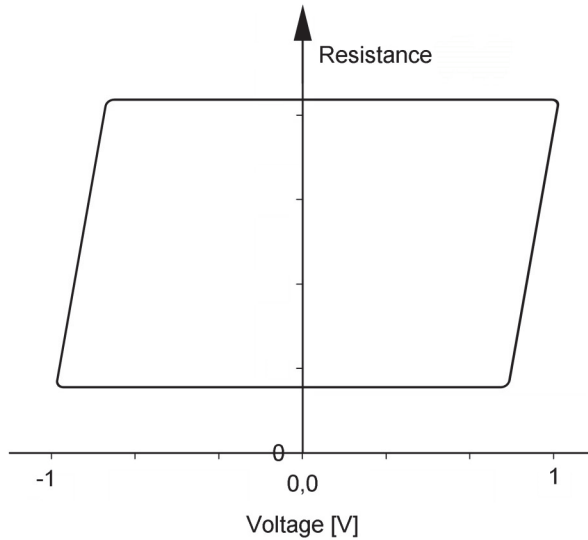
Fig. 3. Schematic hysteretic resistance – voltage behavior of memristor.

The concept of memristors was presented by Leon Chua in 1971 [53] and generalised to memristive systems by Chua and Kang in 1976 [54]. One of the first results describing materials with memristive properties was reported by Argall in 1968, although he described this phenomenon occurring as "a result of trial and error" [55]. It was not until 2008 that Strukov *et al.* were able to combine the discovered hysteretic curves of thin films with the memristor concept [56]. The mechanism of the change in resistance in memristors is due to the drifting of oxygen vacancies towards and away from the metal/metal oxide interfaces [57]. The actual physical mechanism is under continuous study, but evidence has shown that local nanofilaments are responsible for the memristive function [58]. There are numerous predicted applications of memristors. The most obvious application is non–volatile random access memory [59,60], but the memristors can also be used for logic operations [61]. Thus, the same components can be configured to function as either logic gates or memory latches, depending on the need.

Most of the memristor research has been concentrated on inorganic memristor development by thin film deposition techniques, such as nano–imprinting [62] or sputtering [63]. More recently, solutions applicable to the emerging field of printed electronics have been introduced. For example, printed flexible memories using copper phthalocyanine have been introduced by Lian *et al.* where a cross–bar memory was made on polyethylene terephthalate (PET) film by spray coating [64].

27

A sol–gel solution of titanium isopropoxide has been used to produce a memristive layer of titanium oxide by spin coating on the metal bottom electrode [65,66]. Heat–treatments have been used to modify the electrical properties of memristors based on monocrystalline ZnO, achieving very large switching between the "on" and "off" states of the produced components [67]. The influence of heat–treatment on the crystallinity of sol–gel derived TiO_2 has been studied by Tanaka *et al.* [68], but not as a part of memristor research.

3 Materials and methods

This chapter briefly presents the materials and methods used in this work. Because development of formulation methods was an important part of the work, the exact parameters used for each ink are presented in the chapter of results and discussion.

3.1 Materials used in research

All the magnetic inks (Papers I–III) used in this work were based on dry and metallic cobalt nanoparticles produced by Nanostructured & Amorphous Materials Inc. According to the manufacturer's data sheet, they contained 99.8 % of cobalt and were partially passivated with 10 % oxygen. The specific surface area of the nanopowder was determined with Brunauer–Emmett–Teller (BET) surface area analysis based on the physical adsorption of nitrogen gas. The measurement was made with an ASAP 2020 by Micromeritics Instrument Co. for each batch of nanoparticles that was used. Average surface areas varied typically from 17 to 20 m^2/g, corresponding to an average particle size of around 40 nm.

The surfactant used in Paper I was Malialim AAB–0851 from NOF Co. since it contains acid anhydride groups forming a covalent bond with oxidized metal surface of the particles. [69] The adjustment of the rheological properties was done with a N 485 resin solution from Johnson Matthey Plc. The blown menhaden fish oil of grade Z–3 from Richard E Mistler Inc. was used as a binder, due to its ability to polymerize under influence of oxygen. The solvents compatible with the organics were xylene and ethanol (98.5 %, Sigma–Aldrich Co. and 99.9 %, Aa – grade, Altia Oyj).

In Paper II Linoleic acid (> 99 % Sigma–Aldrich Co.) was used both as surfactant and binder and the solvents were terpineol (> 99 %. Merck KGaA) and Aa–grade ethanol (99.5 %, Altia Oyj)

In Paper III Poly(methyl methacrylate) (PMMA) powder with an average molar weight of 350 kg/mol (Aldrich Co.) acted both as a surfactant and binder. Solvents used were 2–(2–Buthoxyethoxy) ethyl acetate (>99.2 %, Sigma–Aldrich Co.) and α–terpineol (>98 %, Merck KGaA). Acetone (99 %, Merck KGaA) was used as a rheology modifier during the milling process.

The piezoelectric ink in Paper IV was based on PZ29 lead zirconate titanate particles from Ferroperm–piezoceramics A/S with an average particle size of 1.2 μm determined with a LS 13320 laser diffraction analyzer from Beckmann Coulter Inc. P(VDF–TrFE) co–polymer, with 56/44 mol.% of each monomer, from Solvay–

Solexis Co. was used as binder material with piezoelectric functionality. Dimethylformamide (>99 %, Fluka Co.) and 2–(2–butoxyethoxy)–ethylacetate (>99 %, Sigma–Aldrich Co.) were used as solvents. As in Paper III, also in this case acetone (99 %, Merck KGaA) was used as a rheology modifier during the milling process.

The TiO_x –precursor solution in Paper V was synthesized at the beginning of the work. On reaction, titanium–di–isopropoxide–2–acetoacetate (75 wt. % in isopropanol, Aldrich Co.) was reacted with 2–methoxyethanol (99.3 %, Aldrich Co.) and ethanolamine (99 %, Aldrich Co). The rheology of the solution was adjusted with isopropyl alcohol (99.5 %, Merck KGaA)

Proper homogenization of the materials was essential for the preparation of the screen printing inks. Both ultrasonic agitation (Hielscher UP 100H, Hielscher Co.) and ball milling (Retsch Co.) were used. A tabletop three–roll mill with steel rolls from Exact Apparatebau GmBH was used for re–milling the inks after storage periods.

3.2 Analysis for the inks stabilized with surfactants

In Paper I and Paper II the particles were coated with a layer of surfactant that made covalent bonds to the particle's surface. The degree of success of the particle coatings was determined using a LEO 912 OMEGA analytical Energy–Filtered Transmission Electron Microscope (EFTEM) (Carl Zeiss SMT AG) to characterize the layers of surfactant on top of the particles before final formulation of the ink. This method, also widely used by others like Ghasemi *et al.* [70] and Garcia–Jimeno *et al*. [71], is a reliable method to visually assess the particle coating due to its high magnification capacity.

The formulated inks of Paper I and Paper II were analyzed with a Netzsch STA 409PC analyzer (Netsch–Geraetebau GmbH) that was able to measure Thermogravimetric and Differential Scanning Calorimetric data as well as Mass Spectrometric analysis of decomposition products (TGA–DSC–MS –analysis). Analysis of the ink in Paper I was carried out in a nitrogen atmosphere (99.995 %, AGA Oy) and in Paper II in a helium atmosphere (99.9995 %, AGA Oy) with a heating rate of 10 °C/min. The analysis enabled the determination of exact solids and volatiles content of the ink adjusted suitably for screen printing.

3.3 Printing experiments

There are many characterization methods that may be used to observe the chemical and physical behaviour of suspensions intended for use as inks. Printing experiments are the most straight–forward method to reveal possible issues of printability, caused usually by evaporation of the solvents. This is the reason why printing experiments were the major method to observe the usability of the ink.

The majority of the inks in this research were made to be used as thicker layers and thus screen printing was the most suitable option. Screen printings were carried out with both manual and machine printing. In the case of memristors, very thin layers were desired and so inkjet–printing was the adopted printing method.

The printer used in the screen printing experiments was a Speedline Technologies MPM Microflex screen printer (Speedline Technologies, Inc.). Printings were done using 10"x10" screens patterned by the author. Both stainless steel and polyester screens with mesh counts of 90, 180 and 320 were used. A typical screen for printing conductive patterns was a 320 mesh stainless steel screen with 16 µm thick emulsion. For magnetic inks both 90 and 180 mesh nylon screens were used with typically 45 µm thick emulsion. Typical force pressing the squeegee against the screen was 2 kg with a printing gap of 0.8 mm.

When the screen printings were carried out manually, a purpose–built jig for the screens was used. The same screens as in the printing machine were used and the jig could be adjusted to the same printing gap as that of the printing machine. The manual force used on the squeegee was determined with test printings.

Memristive material printing tests in Paper V were carried out with a Fujifilm Dimatix DMP–2800 inkjet (Fujifilm Inc) printer using 10–pL droplet printing cartridges. The printings were done on glass substrates coated with two different metal layers to achieve as smooth a bottom electrode surface as possible.

3.4 Analysis of printed patterns

Surface profiler analyses were carried in all the papers. Knowing the exact thickness and thickness variations of the printed pattern is essential for multiple reasons. Firstly, in the evaluation of the electrical performance quality of the printed layer and the material thickness is essential for calculations. Secondly, the layer thickness has a direct influence on the achievable capacitance values or, in the case of piezoelectric component, on the poling process. Thirdly, some components such as memristors require an exact material thickness in order to achieve the desired

electrical properties. The thickness of the printed samples was measured using a Dektak 8 surface profiler (Veeco Instruments Inc). Optical microscopy was also used in combination with surface profilometry. Larger areas were visually inspected to find possible pinholes as these were less likely to be found by the line scan measurement done with the surface profiler.

The Field Emission Scanning Electron Microscope (FESEM) analyses were carried out with Zeiss Ultra Plus and Zeiss Sigma electron microscopes (Carl Zeiss SMT AG). The printed layer analyses were carried out in order to inspect different aspects of the print quality, using both cross–sections of the samples and top surfaces. Both visual inspection and elemental analysis utilizing Energy–Dispersive x–ray Spectroscopy (EDS) were utilized to investigate the distribution of the materials in the layer. Cross–sections were especially used in order to observe the sedimentation of material or agglomeration of particles. In the case of magnetic inks, possible chain formation of particles was considered to be a beneficial phenomenon and thus the possible occurrence of chains was studied.

Possible cracks were observed on both cross–sections and surface images taken with FESEM. Surface images were used especially to find flaws affecting the surface quality of printed patterns such as pinholes, cracks or lumps of agglomerates. Especially with memristors the surface images were a useful method to observe the deterioration of the material during treatments.

3.5   Adhesion experiments

Two types of adhesion tests, pull–off and tape–peel tests, were carried out on the samples reported in Paper III and Paper IV. The pull–off tests were done using a PosiTest AT–A –tester (De Felsko Co.) and the tape–peel tests with an Elcometer 107 X–Hatch kit (Elcometer Ltd.) according to the ASTM D–3359–B cross–hatch test.

The pull–off test (Figure 4) was a feasible method to see the overall adhesion of the layer on the used substrate and to get quantitative information about the adhesion. In tests, $\varnothing$20 mm aluminum dollies were glued to the printed and cured ink layers and the tests were carried out on the following day using the tester to pull the dolly from the surface. The tester measured the force needed to detach the dolly from the sample. Three to four parallel measurements were done and the average result was calculated.

The tape–peel test was especially used for testing the integrity of the printed and cured layer. On the test carried out according to the standard, three cross–cut

patterns were cut into the printed surface with a tool consisting of six parallel blades. Each pattern consisted of 25 small squares of ink that were cut all the way to the substrate. Tape was glued on top of the cut pattern and peeled off. The integrity of the squares was investigated before and after peeling. If the adhesion was sufficient, the squares remained intact. Figure 4 shows two typical samples resulting from the pull–off and tape–peel tests.

A.   B.
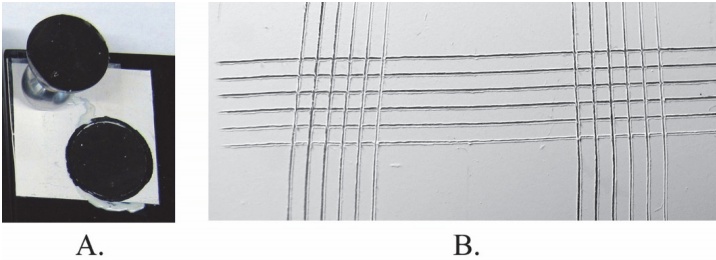
Fig. 4. A: Pull–off test sample with peeled off aluminum dolly. The failing material was in this case the substrate. B: Two cross–hatch patterns cut for the tape–peel test. No squares from patterns were peeled off.

4 Results and discussion

4.1 Formulation of inks

The majority of this work concentrated on the formulation of screen printing inks for different applications based of different inorganic materials. The novelty of the screen printing inks produced was to use dry powder as a raw material for the production of low temperature curing inks. Another part of this work was the development of an inkjet printable memristor. A new synthesis route was developed and the resulting solution was formulated into inkjet printable form. A short summary of the different inks made in this work is presented in Table 2 and their process flow is shown in Figure 5.

Table 2. The composition of inks made in this work.

Paper	Type	Vol.% filler	Filler	Binder	Surfactant
I	Magnetic	10, 14, 21	n-Co	Fish oil	AAB-0851
II	Magnetic	50	n-Co	Linoleic acid	Linoleic acid
III	Magnetic	30, 40, 50, 60, 70	n-Co	PMMA	PMMA
IV	Piezoelectric	30, 40, 50, 60, 70	PZ29	PVDF/TrFE	None
V	Memristor	n/a	TiOx	None	None
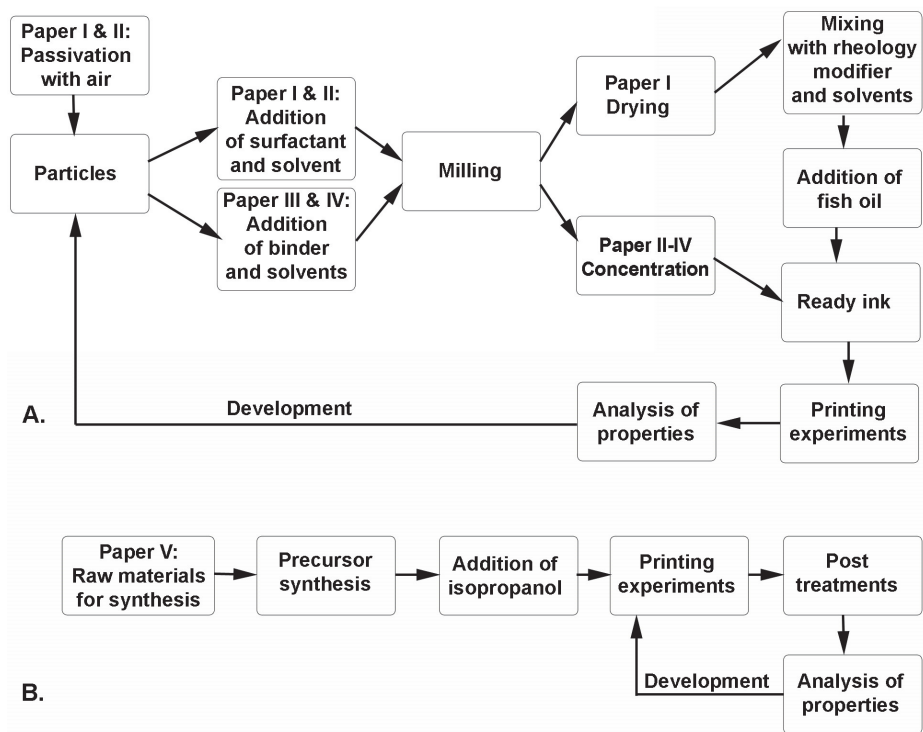
Fig. 5. A: Process flow of the ink formulations on Papers I–IV. B: Process flow on Paper V.

During the research and optimization of the ink formulations in this work, one about 20 ml batch of each ink shown in the Table 2 were prepared, except in the case of the piezoelectric ink with 50 vol. % filler addition due to the large quantity of samples needed for the polarization tests. It is clear that further studies are required when the optimized inks are to be utilized in practical applications with large quantities. Several samples (3–20) per formulated ink were prepared for each characterization methods. All the inks had good and stable properties during the printing and thus the selection of the most feasible ink compositions was performed according to the quality of the cured layers. The inks formulated in the Papers I–III and V remained printable over one year.

4.1.1 Utilization of surfactants

The first task in the screen printing ink formulations was to investigate the stabilization of the formulated magnetic inks with different surfactants, which enabled the formulation of magnetic inks directly from dry nanoparticle powder. Applying a surfactant coating to the particles greatly reduced their agglomeration. Agglomeration leads to irreversible sedimentation, the phenomenon that eventually makes the ink unprintable.

The quantity of surfactant needed can be determined on the basis of the molecular weight of the functional unit, such as a fatty acid molecule or the repeating unit of a polymer, if the specific surface area of the particles to be coated is known. Since the surface area covered with a single fatty acid molecule was 0.21 nm^2 and with an acid anhydride group 0.45 nm^2 [69], the quantity needed for a single molecular layer could be calculated accurately.

The first ink in this work was made by utilizing a commercial polymeric surfactant containing acid anhydride groups [Paper I]. It was used with the addition of menhaden blown fish oil to work as a binder and a commercial rheology modifier to enhance the printability of the ink. A filler contents of up to 70 wt.% (22 vol.%) was achieved.

In Paper II the idea of utilizing the surfactant both as a stabilizing agent and binder was successfully investigated. An oxidatively polymerizing fatty acid, linoleic acid, was used for this task. The ink formulated in this paper remained printable for two years when stored at room temperature. It also proved to have good electrical characteristics as reported in two articles. [Paper II] [72] The filler content of the ink was also greatly enhanced, being 88 wt.% (50 vol.%) for the ink with good printing characteristics.

In Paper III the ink was stabilized by ball–milling the cobalt particles with the PMMA polymer, working both as a binder and stabilizer. The change of binder was made in order to achieve good adhesion to the polycarbonate (PC) substrate. The solids content of the ink with the best adhesion and electrical properties was also in this case achieved with 50 vol.% of Co, as in Paper II. Higher solids contents up to 70 vol.% were tested but proved to have low adhesion after curing.

4.1.2 Commercial acid anhydride surfactant

Polymeric surfactant Malialim AAB–0851 (Figure 6) from NOF Co. was used for surface treatment of the cobalt powder [Paper I]. The reactive part of the polymer

is a carboxylic acid anhydride group capable of forming a covalent bond to the surface of the metal particles. The weight of the repeating unit of the polymer was 968 g/mol, which was calculated from the material's saponification value of 95 mg KOH/g surfactant. The repeating unit of the backbone polymer had two side chains, where one consisted of polyethylene oxide and the other of polystyrene, in order to improve the solubility of the material.
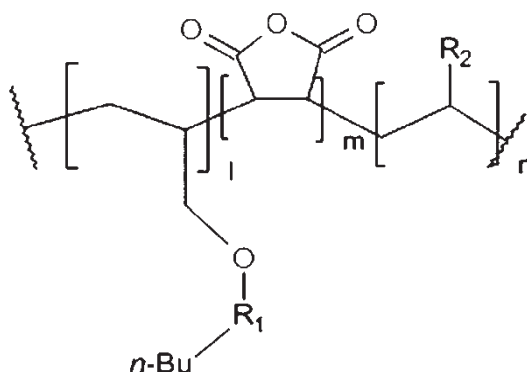

Fig. 6. The chemical structure of surfactant (Malialim AAB–0851) used in Paper I, where R1 is polyethylene oxide and R2 is polystyrene. The acid anhydride group made covalent bonds with the cobalt particles. Reproduced courtesy of The Electromagnetics Academy. [Paper I].

The development of the ink started with the surface treatment of the cobalt nanoparticles by adding them into a solution of Malialim surfactant and xylene. The solution was mixed in a ball mill using a nylon pot and agate milling balls. After 16 h of milling, the solution was placed in a furnace and the xylene was evaporated at a temperature of 80 °C for 24 h.

The resulting material was analyzed with EFTEM to characterize the layers of surfactant on top of the particles. Firstly 0.2 g of surface treated particles was washed twice with 10 ml of ethanol to remove the excess of unreacted polymer material. The ethanol was removed with a 0.2 μm PTFE filter. The particles were collected and dried at room temperature for 24 hours before the analysis.

For the analysis, 0.1 g of washed particles was dispersed in 20 ml of acetone using an ultrasonic bath. A 5 μl droplet of dispersion was placed on a TEM grid and the solvent was evaporated. A semi–transparent layer of surfactant could be observed on EFTEM analysis. Since incorrect focusing of an EFTEM also causes

the appearance of a similar kind of visual distortion at the particle edges a particular care was taken to achieve correct focusing. An example of particles with a 5 nm thick surfactant layer imaged by TEM is shown in Figure 7.
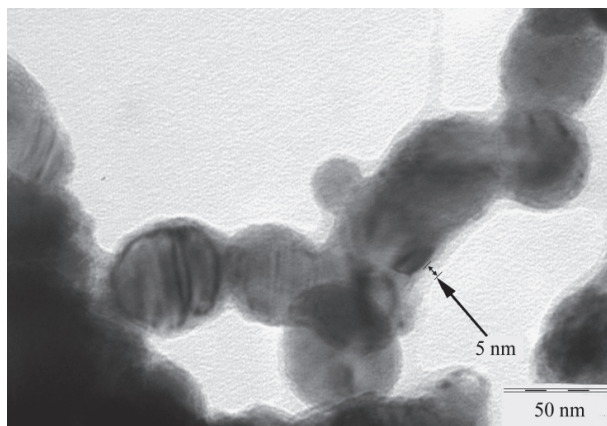

Fig. 7. The polymeric surfactant layer with a thickness of approximately 5 nm on the surface of the Co particle chains. Reproduced courtesy of The Electromagnetics Academy. [Paper I].

4.1.3 Fatty acid as surfactant/binder

The fatty acids are an interesting group of materials utilized for stabilization of nanoparticle suspensions. This is due to their ability to act both as a capping molecule during nanoparticle synthesis [73] and as a stabilizing agent in the nanoparticle suspensions [74, 75]. In addition, unsaturated fatty acids have the capability of reacting with cross–linked polymeric structures when exposed to oxygen [69, 76]. Their carboxylic acid group can also make a covalent bond to metallic surfaces (such as copper antenna patterns) [69]. The combination of these properties makes them useful both as surfactants and binding materials

Linoleic acid is an unsaturated fatty acid and is a major component of linseed oil. Linseed oil has been used as a binding material on traditional paintings due to its capability to polymerize (i.e. dry) with reactions occurring between its double bonds and oxygen. [77] Since these reactions are known to be catalyzed with transition metals such as cobalt and zirconium [76] it was interesting to experiment with its use in magnetic ink applications.

Some of the reactions occurring during oxidative drying of the oil are presented in Figures 8–11. The reactions start with scission of a single α–hydrogen from between the double bonds of the molecule chain as presented in Figure 8. [78] This can occur due to interaction with a metal, due to UV–light or a radical initiator formed earlier. The formed radical is stabilized by resonance taking place between the π–electrons of the double bonds. The initiation is clearly the slowest phase of the reactions and propagation reactions carried out by resulting radicals occur much more rapidly. [77, 76]
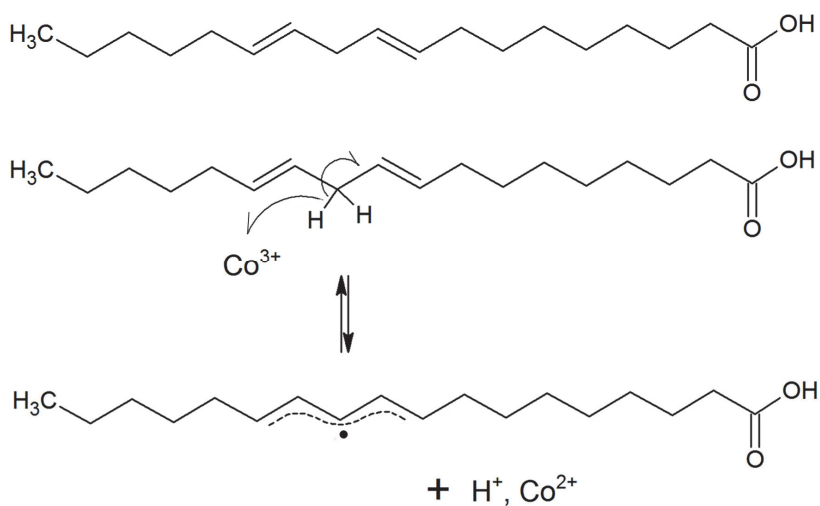
Fig. 8. Structure of linoleic acid (top) and radical forming reactions due interaction with cobalt (middle and bottom). [78].

The formed Co^{2+} cation can further react with oxygen and a released a proton, resulting in a more reactive singlet state oxygen, peroxide radical and a Co^{3+} cation that can react again with another fatty acid chain. [76] This makes cobalt an excellent catalyst for fatty acid polymerization. Both the stabilized radical in the fatty acid chain and the exited structures formed with oxygen can take part in propagation reactions. Figures 9 and 10 show some of the propagation reactions occurring with the radical formed on the fatty acid chain. The peroxide structure formed in Figure 10 is thermodynamically unstable and will react further to form two radicals. [77–79]
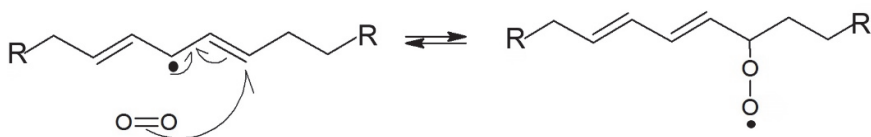
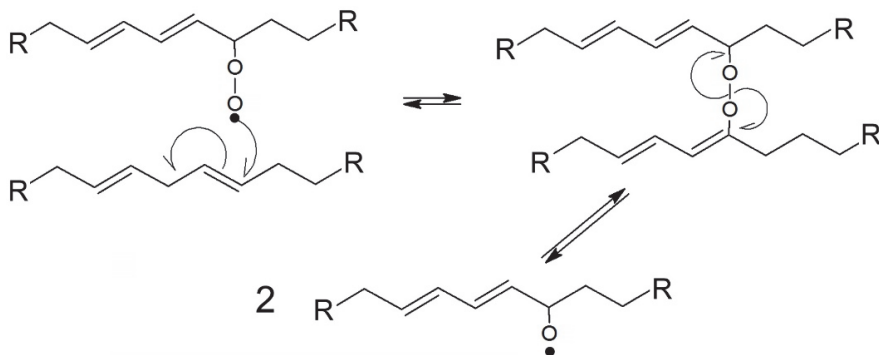Fig. 9. Oxidation reaction of the radical formed by catalyst. [77–79].

Fig. 10. Typical propagation reactions occurring during oxidative polymerization of fatty acid. Formed peroxide structure decomposes into two radicals. [77–79].

A typical termination reaction is presented in Figure 11. The radical can also form directly into a carbon chain, resulting in a carbon–carbon bond between the fatty acid chains. [79]. Peroxide structures between the fatty acid chains can also be formed during the termination reactions, although they will further react into a more stable form over time. The resulting dried fatty acid will eventually be full of cross–linked molecular chains that are also bound to metal surfaces with their carboxylic acid groups. This makes the adhesion of the formulated ink very strong, as was also noted during the work.
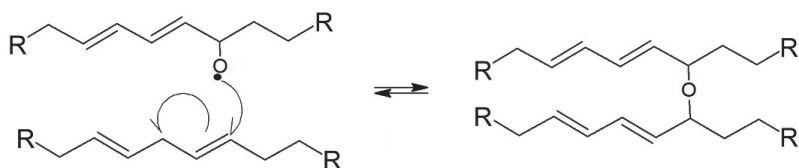

Fig. 11. Termination reaction forming ether–type oxygen bonding between two fatty acid chains. This type of bonding finally results in cross–linked structures between fatty acid chains.

41

The required amount of linoleic acid for surface coating of the particles was calculated on the basis of the specific surface area of the powder determined with BET adsorption isotherm analysis. 1.9 g of the acid was needed for coating 50 g of nanoparticles. In addition to the calculated value, 5.3 g of linoleic acid was added to improve the rheological properties of the ink during printing and to act as a binding material on the metal surfaces. The additional amount of fatty acid was decided on the basis of printing experiments.

The linoleic acid was dissolved in ethanol after which dry cobalt nanoparticles were added into the resulting solution. The suspension was homogenized with ultrasonic agitation at 30 W for 30 s. The suspension was then milled in a ball mill using a nylon cup and agate milling balls at moderate speed for 16 h in order to break up the agglomerates formed by the nanoparticles. After milling, the solvent was evaporated at 90 °C for 16 h in a nitrogen atmosphere in order to avoid oxidative polymerization of the surfactant.

The nanoparticles were analyzed with an EFTEM microscope to observe the attachment of fatty acid surfactant layers on top of the particles. First, 0.2 g of surface treated particles was washed three times with 10 ml of ethanol to remove the free fatty acids. During the washing, the particles were mixed with ethanol, the solution was settled by using a centrifuge, supernatant ethanol was removed and the washing procedure was repeated. Finally, the EFTEM analysis sample was prepared by dispersing the particles in acetone. Thus it was certain that only fatty acid bound to the particles' surface was present. On analysis a clear semi–transparent 8 nm thick layer of the linoleic acid could be observed on the surfaces of the particles, as can be seen in Figure 12.
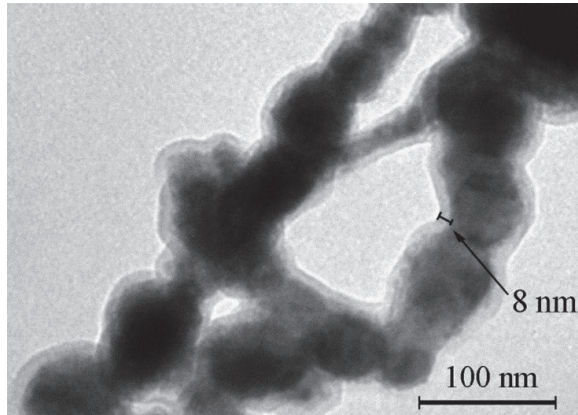
Fig. 12. Cobalt nanoparticles with linoleic acid coating. Typical thickness of the organic layer was 8 nm. Reproduced courtesy of The Electromagnetics Academy. [Paper II].

4.1.4 Poly(methyl methacrylate) as binder

The cobalt based inks produced in Paper I and Paper II were made for antennas with a radiation pattern of copper on which the inks had good adhesion. However, in Paper III the substrate material used for the antenna was changed to PC. In order to achieve a cobalt based ink suitable for the flexible PC substrates, a different binder material was needed. PMMA was reported earlier to be a reliable binder material for flexible applications [80], and also for severe conditions [81]. Since the solvents suitable for PMMA are similar to those for PC, a good adhesion could be expected.

   Due to the reactivity of the particles, the dry powder was handled under a nitrogen atmosphere while being submerged into the acetone used in the milling solution. PMMA powder with an average molar weight of 350 000 g/mol was added into the acetone solution together with 2–(2–Buthoxyethoxy) ethyl acetate. Five ink batches were made, consisting of 30–70 vol.% (77–95 wt.%) of cobalt particles in dry solids, all of them containing 10 g of particles. The suspensions were mixed in a planetary ball mill using a nylon pot and agate milling balls.

4.1.5 Magnetic inks based on commercial surfactant coated particles

The inks in Paper I were made on the basis of the particles described in Chapter 4.1.2. A base ink was formed by ball–milling 50 g of coated particles with 56 g of

Johnson Matthey N485 solution and 55 g of ethanol to lower the viscosity. A homogenous paste resulted after milling for 24 h. The TG–DSC–MS analysis was carried out for the base ink sample before concentration to printable viscosity in order to determine the exact solids content of the Johnson Matthey solution. As shown in Figure 13 the solvents were first evaporated from the sample after which at 400 °C the solid organic material decomposes, as indicated by the rapid downward peak and the declining weight of the sample weight. This was also detectable as an endothermic peak in the calorimetric measurement data. Additionally the mass spectrometer data (Figure 14) at mass number 12 (carbon) revealed that the weight loss was due to organic material decomposition.
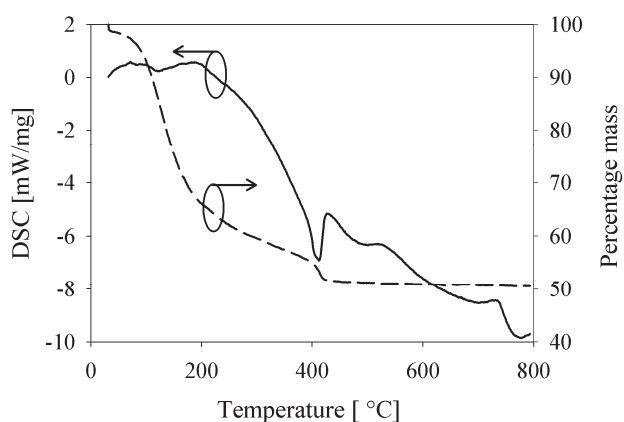
Fig. 13. TGA and DSC signals for TG–DSC–MS analysis for the cobalt ink with N485 solution and ethanol. Dashed line presents changes of mass and solid line DSC signal. Majority of solvents are removed below 200 °C. At 400 °C the decomposition of the solid organic material occurs, indicated by both signals. Reproduced courtesy of The Electromagnetics Academy. [Paper I].
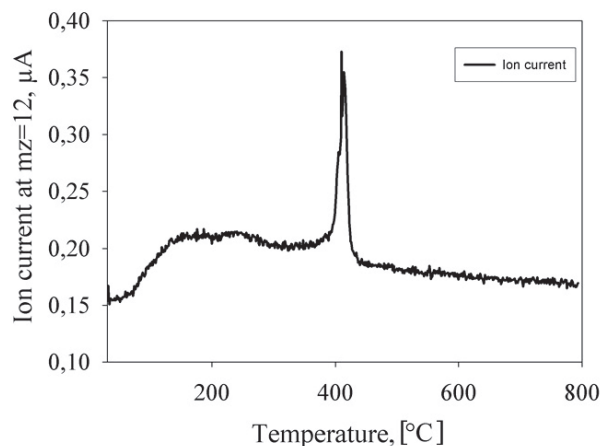
Fig. 14. Mass detector signal at mass number 12 from the TG–DSC–MS analysis of the cobalt ink without menhaden oil in Paper I. Strong increase in signal can be seen at the temperature of rapid weight loss indicating the polymeric carbon breakdown. Reproduced courtesy of The Electromagnetics Academy. [Paper I].

The viscosity of the base ink was increased by evaporation of the solvents until printed parallel line test patterns with linewidths of 250, 500 and 750 μm achieved a homogenous print quality. Solid printed lines without excess spreading of the ink and good ink transfer through the printing screen were found to be of the best quality when the ink contained 25 wt.% of volatiles, 60 wt.% of cobalt and 15 wt.% organic solids. The proportion of the volatiles and solids was determined by gravimetrical analysis from the printed test patterns. Printings were done using 325 and 230 mesh nylon screens with 16 μm and 30 μm emulsion thicknesses.

Menhaden oil was added to the base ink in different quantities to determine the most suitable amount of binding material. Samples consisting of 50, 60 and 70 wt.% (10, 14 and 21 vol.%) of Co in the dry solids contents were achieved. The developed inks were analysed with a cone and plate rotation rheometer. The change of viscosity caused by the addition of binder material to the samples (Figure 15) showed a significant decrease in viscosity between the 70 wt.% and 50 – 60 wt.% solids samples, which also affected the quality of the printed patterns. This will be further discussed in the print quality analysis chapter.

Viscosity measurements were not carried out in the latter part of the thesis. The most suitable printing viscosity of the ink is highly dependent on the nature and quantity of the binding material. If the binder content is high, typically a lower viscosity is needed due to the fact that the binder starts to precipitate out from the

45

ink when the solvent/binder proportion is too low. A suitable viscosity for each ink is thus found through printing tests and visual inspection.
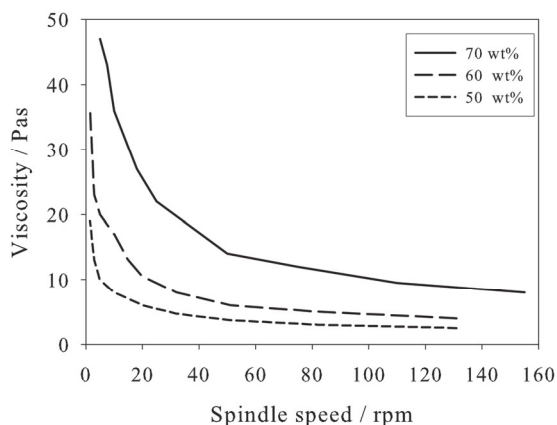

Fig. 15. The viscosity of ink samples of Paper I as a function of spindle speed with different amounts of cobalt. Reproduced courtesy of The Electromagnetics Academy. [Paper I].

4.1.6 Formulation of magnetic ink based on fatty acid coated particles

In Paper II the ink formulation process was further simplified based on experience gained during the research reported in Paper I. It was noted that an ink containing 12 wt.% linoleic acid and 88 wt.% (50 vol.%) cobalt as dry solids had the most suitable characteristics in the printing tests. The printings were done using a 180 mesh nylon screen and an emulsion thickness of 30 µm.

DSC–TGA–MS analysis was used to determine the exact composition of the ink most suitable for screen printing. The measurement was carried out in a helium atmosphere in order to avoid oxidative reactions of linoleic acid (Figures 16 and 17). During the measurement, it was also observed that a small portion of the ink decomposed at 170 °C, indicated by a weight loss and the release of carbon due to decomposition of organic material. This was most likely caused by unstable organic structures formed in the surfactant due to oxidative polymerization reactions occurring during the ink sample manufacture.

46
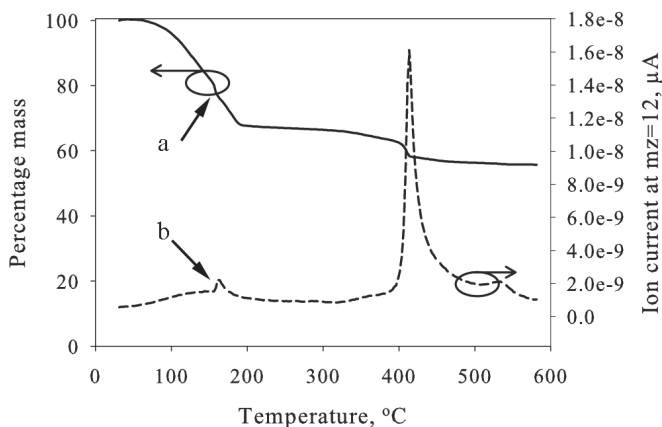
Fig. 16. Thermogravimetric (solid line) and mass spectrometer data at mass number (mz) = 12 (dashed line) of the cobalt ink sample analyzed in He atmosphere. Arrow (a) points out the loss of mass due to decomposition of organic material at temperature of 170 °C, also observed in the mass spectrometer signal (arrow b). Reproduced courtesy of The Electromagnetics Academy. [Paper II].
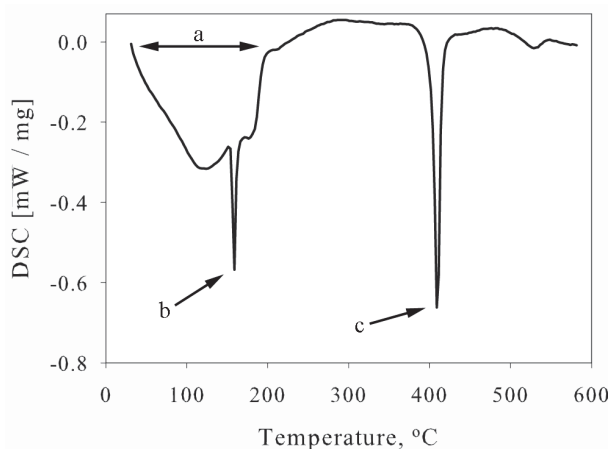
Fig. 17. DSC data of the Co ink sample. Arrow (a) shows the temperature range of evaporation of solvents. Arrow (b) points out the consumption of energy caused by thermal decomposition of organic material observed also in the thermogravimetric and mass spectrometric measurements. Arrow (c) points to the signal caused by the thermal decomposition of surfactants. Reproduced courtesy of The Electromagnetics Academy. [Paper II].

4.1.7 Formulation of poly(methyl methacrylate) stabilized magnetic ink

The formulation process for PMMA stabilized magnetic inks was simplified even further on the basis of the earlier experiments. As a starting point, the desired amount of PMMA and Co were known and could be weighed for the milling process. Thus the main task was to concentrate the milled ink by evaporating the solvents in order to achieve good rheological characteristics for printing. On concentration the milled suspensions were placed in decanter flasks heated with a heating plate with constant stirring by a drill mixer. The evaporation of the solvents was aided by nitrogen flushing. During evaporation, 10 ml α–terpineol was added to each suspension in order to adjust the drying characteristics of the ink. When the viscosities of the solutions were high enough for screen printing, the ink samples were collected into air–tight containers and cooled down.

4.2 Formulation of piezoelectric inks

The piezoelectric inks made in Paper IV were based on piezoelectric polymer, P(VDF–TrFE), and piezoelectric lead zirconate titanate ceramic PZ29 without surfactants. In this approach the main target was to investigate if piezoelectric performance could be achieved with layers fabricated by printing inks with a simplified formulation, although it could be predicted that the stability of the inks would be compromised.

The preparation was started by dissolving the P(VDF–TrFE) co–polymer powder into dimethylformamide, which resulted in a clear 20 wt.% solution for further experiments. Of each ink batch produced, 10 g of PZ29 was used and P(VDF–TrFE) solution was added in order to prepare five solutions containing 30, 40, 50, 60 and 70 vol.% of PZ29 in dry solids. With each batch, 10 g of 2–(2–butoxyethoxy)–ethylacetate was used as a secondary solvent to improve the drying characteristics of the ink. 20 ml of acetone was added to each batch in order to reduce the viscosity for the ball milling.

The inks were prepared in a ball mill using nylon milling jars and agate milling balls for 18 h in order to de–agglomerate the raw material. After milling the viscosity of the inks was adjusted for printing by evaporating the acetone and concentrating the resulting inks using a drill mixer and a heating plate. The inks were collected and used for printings within a day of preparation because to their tendency to sediment. Printings were done manually using typically a 90 µm thick

stencil and a doctoring blade. If longer storage was needed, the inks were re–mixed using a three–roll mill with stainless steel rollers.

4.3   Sol–gel synthesis and inkjet printing for memristive solution

The synthesis of a TiO_x –precursor solution was based on the works by Kim *et al.* [82] and Gergel–Hackett *et al.* [65]. However, instead of using titanium(IV)isopropoxide as in the references, more stable [83] titanium–di–isopropoxide–2–acetoacetate was prepared as a precursor by mixing it with 2–methoxyethanol and ethanolamine in a round–bottom flask equipped with a thermometer, nitrogen inlet and condenser. The flask was heated in an oil bath and the reagent solution was constantly stirred with a magnetic stirrer. After the reaction, the resulting solution was collected, cooled and stored in a refrigerator at 5 °C. A solution for inkjet printing was prepared by diluting the TiO_x –precursor with isopropyl alcohol.

The printing tests using an inkjet printer were carried out on glass substrates coated with two different metal layers to achieve as smooth a bottom electrode surface as possible. The RF – sputtered metal layers used were a 100 nm thick silver layer on the bottom and a 20 nm thick titanium or copper layer on the top. Titanium was chosen due to possible positive interaction between the memristive layer and metallic titanium [63]. Copper was chosen in order to investigate the possibility of using inexpensive copper ink in the future in fully inkjet printed memristors. The silver layer was used due to its good adhesion and rapid sputtering.

After printing, the resulting patterns were kept in air at room temperature for 60 min allowing the hydrolysis reactions to occur in the TiO_x pattern [82]. After the reaction, the volatiles were evaporated by heating the sample to 150 °C in a nitrogen atmosphere for 10 min, followed by the electrical measurements. A batch of samples was set aside for additional heat–treatments in an argon atmosphere for one hour to investigate its influence on the resistance values and lifetime of the memristors. The temperatures used were 250, 300, 350, 400 and 450 °C.

4.4 Analysis of printed patterns

4.4.1 Surface profiler analysis

In Paper I, the printability and printing accuracy of the produced ink was investigated by making test prints with 500 μm lines through a 230 mesh polyester screen. The surface profiler analyses (Figure 18) were carried out on different inks. The results indicated that decreasing the metal content from 70 wt.% down to 50 wt.% enabled smoother surfaces and better defined printed patterns. Later work carried out with other cobalt inks with different formulations, [Paper II], [Paper III], revealed that a much higher metal content (~88 wt.%) could be achieved while still retaining good quality printing according to the FESEM analysis.
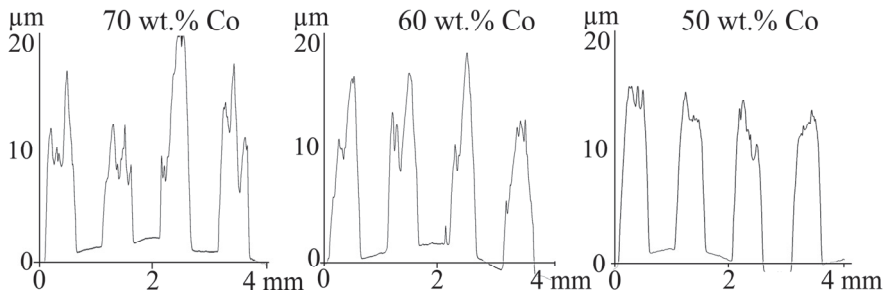
Fig. 18. Profiles of the screen printed lines containing 70–50 wt.% of cobalt. Lower metal content enables smoother surfaces and better defined patterns. Reproduced courtesy of The Electromagnetics Academy. [Paper I].

The surface profiler analysis in the Paper II was carried out on cobalt ink samples that were printed on patch antennas patterned on copper foil on a FR4 printed circuit board. The result presented in Figure 19 indicated that the ink did not completely level before curing. It could be concluded that the long period variation (2 mm peak to peak) of the pattern was caused by the structure (glass fibre bundles) inside the FR4 substrate. The short period variation (100 μm peak to peak) was due to the screen. It was further concluded that a slight increase in the amount of binding material would be beneficial for the surface quality. In addition to this, slower drying of the printed samples would have a positive influence on levelling the printed patterns.
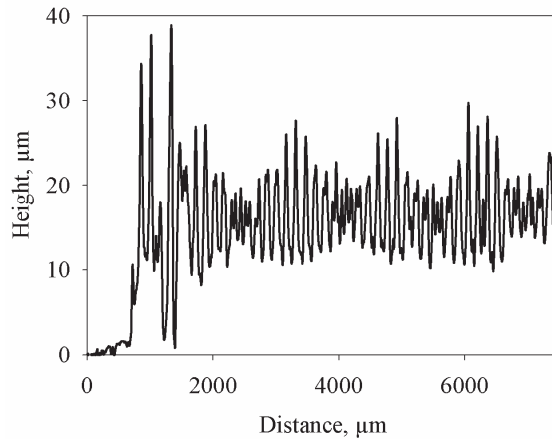
Fig. 19. Measured surface profiles of single printed magnetic layer on patch antenna. Reproduced courtesy of The Electromagnetics Academy. [Paper II].

In Paper V, the surface profiler was used in order to observe the thickness of areas with memristive functionality. In order to find such areas, electrical measurements were carried out with a probe station using a sourcemeter to measure current–voltage (I–V) curves. Measurements were carried out at ambient temperature and normal atmosphere by placing one probing needle directly on top of the memristive layer and another on the bottom electrode. Utilizing direct probing instead of top electrodes was done due to the observation that there was no memristive functionality on samples with top electrodes larger than 50 µm. Due to the possibility to investigate larger areas in short time, direct probing was found out to be the most efficient way for the measurements. If all–printed memristive devices are desired, there is a clear benefit for making the lateral size of the component as small as can be achieved with the used manufacturing method.

In the measurements, 100 ms voltage pulses from –0.4 to 0.4 V or –0.6 to 0.6 V with 0.1 V increments were fed to the samples and changes in resistance values were calculated. Areas with memristive functionality were marked during the measurement and the thicknesses of the areas were analysed with the surface profilometer. Figure 20 shows surface profiler measurement result on a memristive area. Optimal memristive functionality was achieved when the thickness of the layer was in the range of 70–80 nm. Areas with thickness greater than 100 nm did not exhibit memristive properties. On the other hand, areas thinner than 50 nm were not able to withstand even one read–erase–cycle.

51
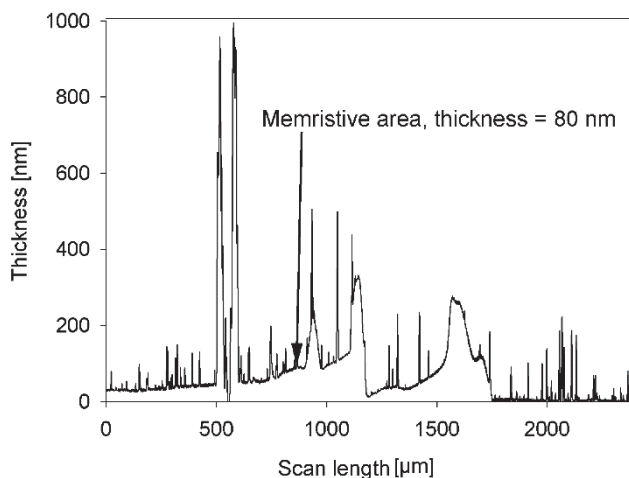
Fig. 20. Surface profiler measurement showing a memristive area marked with an arrow. The bottom electrode starts at 1700 μm. Copyright (c) 2013 The Japan Society of Applied Physics [Paper V].

Stencil printing was used for the cobalt inks in Paper III and for the piezoelectric inks in Paper IV, which resulted in surfaces already levelled during the printing process. However, the surface profilometer was used to observe the thickness of resulting printed layers.

4.4.2 FESEM–analyses of printed patterns

FESEM analysis was utilized in all publications referred to in this thesis. Electron microscopy was used to observe the print quality of screen printed layers in Papers I–IV, especially the cracks and agglomerates on the inks. Backscattering images were used to investigate the filler distribution in the polymer matrix. Cross–section images of printed patterns revealed possible sedimentation of the particles as well as agglomeration of fillers, cracks within the layer and possible peeling of the layer. With memristors the FESEM analysis revealed the effects of heat–treatments, such as peeling or diffusion of the bottom electrode materials [Paper V].

The magnetic inks produced in Paper I proved to contain a lot of minor agglomerates, clearly indicating a need for further ink development. Figure 21 shows the FESEM images from cross–sections of printed patterns with different ink compositions on PET film. The backscattering images with a magnification of 1000 x indicate no sedimentation of the cobalt occurring during the drying of the

ink layers. However, the agglomeration of the particles clearly increased as a consequence of higher cobalt content. The horizontal cracks in the sample with 70 wt.% of cobalt were most likely caused by the casting process of the SEM samples, as well as the peeling of the printed layers from the PET in all samples. The secondary emission images with a magnification of 100 000 x are shown in the inserts. It can be observed that in samples containing 60 and 70 wt.% of Co, the nanoparticles are more visible and also self–arranging in lines, whereas in the 50 wt.% sample the particles are mostly submerged in the binding material.
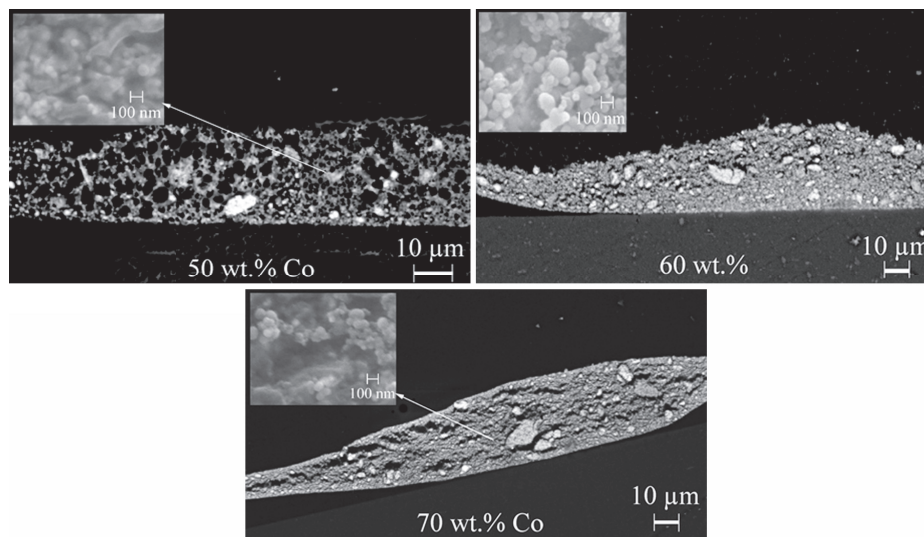
Fig. 21. Backscattering (1000 x) and secondary emission (100 000 x) FESEM images of cross–sections of cobalt inks printed on PET. Reproduced courtesy of The Electromagnetics Academy [Paper I].

The ink reported in Paper II proved to be more homogeneous than those in Paper I. The FESEM analyses in general revealed that the nanoparticles in the printed patterns were well dispersed. Only a few small agglomerates were visible, proving that the linoleic acid was a more efficient surfactant in this case where cobalt nanoparticles were used. Also, printing experiments carried out one year later with the produced ink that had been kept in a sealed container at room temperature proved that the ink could remain non–sedimented over a long period of time.

Figure 22 shows a backscattering image from a cross–section of the patch antenna with five printed layers of ink. The ink was able to cover all the unevenness

of the copper surface, indicating good wetting. A few minor cracks in the printed patterns were visible, indicating that a slight increase in linoleic acid content would be beneficial when an especially smooth print quality is needed. Overall it can be concluded that the ink developed in Paper II exhibited greatly improved properties with a much higher metal content (88 wt.%) when compared to the inks produced (up to 70 wt.%) in Paper I.
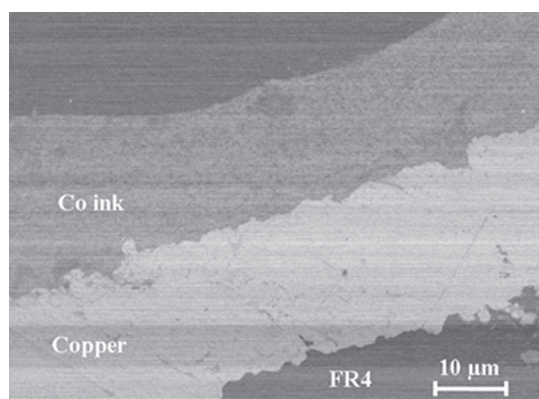
Fig. 22. Backscattering image from cross–section of patch antenna with five printed layers of Co ink. Reproduced courtesy of The Electromagnetics Academy [Paper II].

The layers printed on PC sheets in Paper III were analyzed using backscattering FESEM images with 50 000 x magnification (Figure 23). The cross–section images (Figure 23 A–E) show that the cobalt nanoparticles were well dispersed into the polymer matrix, until the loading level reached 60 vol.% and the particles started to agglomerate. The increase of the cobalt content also enhanced self–arrangement of the particles into chains, clearly visible in the image taken from the surface of the sample containing 60 vol.% Co (Figure 23 F). Also, the increased porosity caused by the agglomeration of the particles indicated that the amount of polymer was no longer enough to form a uniform matrix.
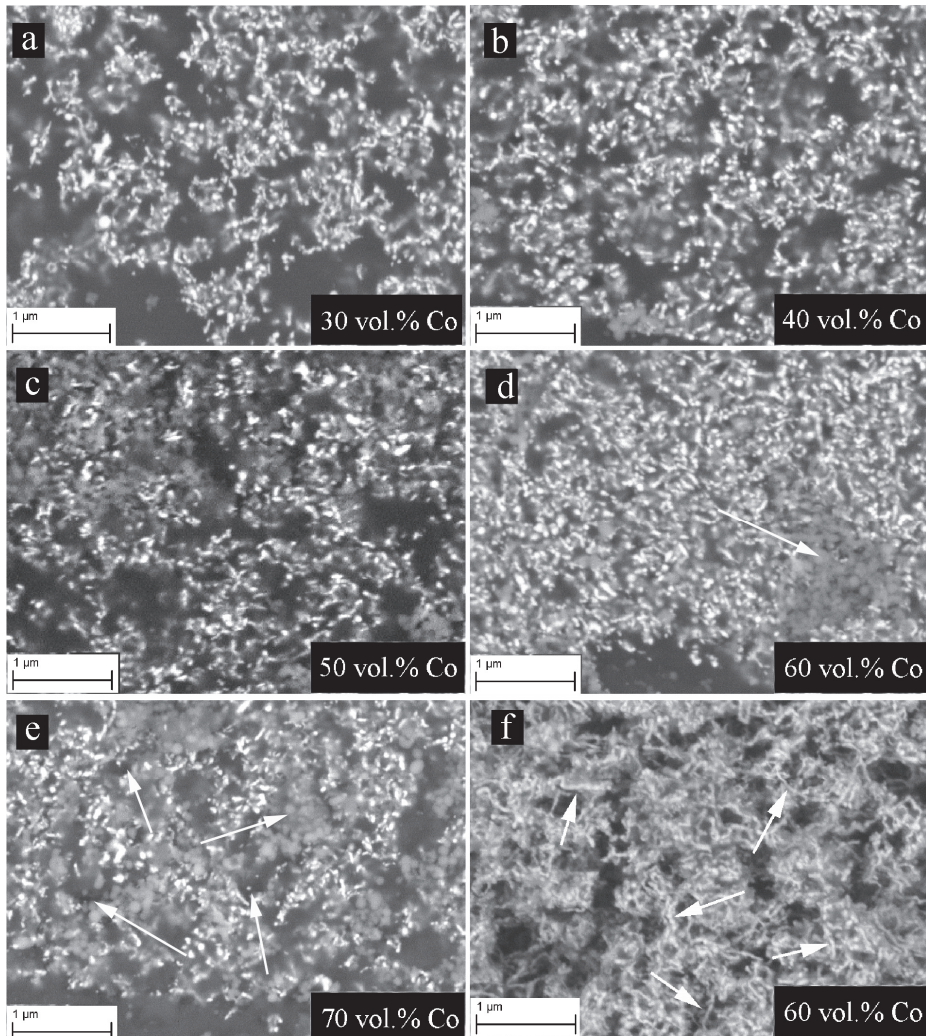
Fig. 23. FESEM backscattering images of the samples. Cobalt can be seen as brighter areas on transparent polymer phase. a–e: images of cross–sections of the samples reveal increasing porosity of the samples (marked with white arrows) as cobalt content increases. f: image on the surface of the sample consisting 60 vol.% cobalt shows lines formed by cobalt nanoparticles. Copyright 2015 by The Minerals, Metals & Materials Society. [Paper III].

The particles contained in the piezoelectric inks in Paper IV were much larger in size (1–3 μm) when compared to magnetic inks that contained only nanoparticles.

Thus the possible agglomeration of materials and voids in the printed pattern was much easier to observe on FESEM analysis.

The backscattering images of the printed layers (Figure 24) taken from the surface of the samples show that the PZT particles were evenly scattered inside the partly transparent P(VDF–TrFE) phase. When the amount of the PZT particles increased to 60 vol.%, holes and pores could be observed, indicating that the quantity of P(VDF–TrFE) was not enough to fill all the spaces between the particles. Also, as the relative amount of the polymer declined, the agglomeration of the particles slightly increased.
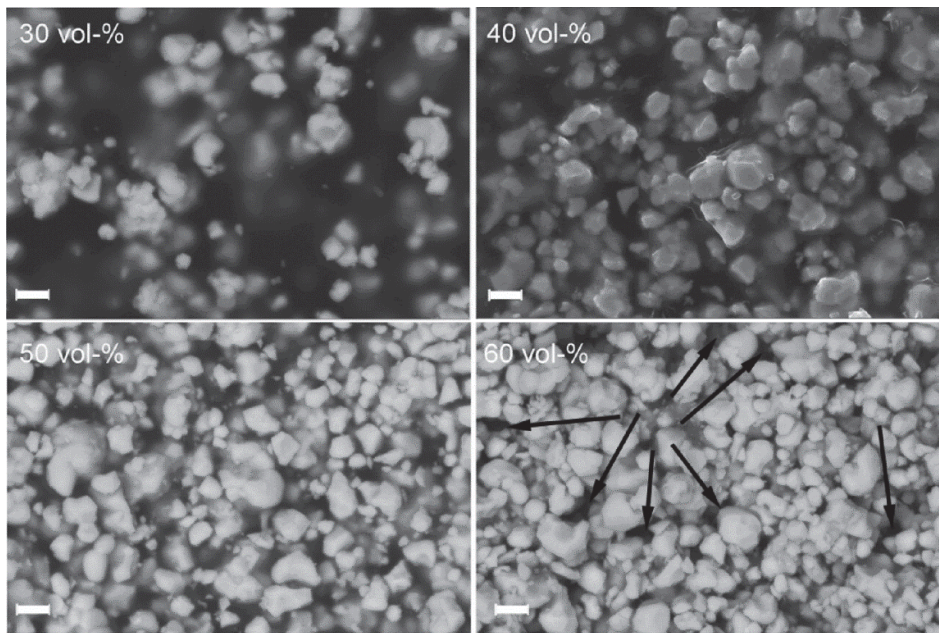
Fig. 24. Backscattering FESEM images of the surfaces of the printed PZT/P(VDF–TrFE) patterns with different loading levels of PZT particles. Magnification = 20 000 x, scale bar = 1 µm. Porosity can be clearly seen in sample containing 60 vol.% of PZT (pores marked with black arrows). A slight increase in the amount of agglomerates and particle–to–particle contact level as a function of ceramic content in the ink was observed. Copyright 2015 Elsevier. [Paper IV].

Overall, the ink with 60 vol.% of PZT had increased particle–to–particle connectivity. The percolation of filler in the composites having more than 50 vol.% of ceramic particles has also been seen in some other P(VDF) composite studies

[84–86]. The ink containing 70 vol.% of PZT particles was discarded from the FESEM studies due to its lack of electrical properties. No functional samples could be printed with this ink due to the cracks and pinholes appearing in the printed and cured patterns caused by the relatively small quantity of the binding polymer material.

All memristive film samples in Paper V were analysed with FESEM in order to investigate the changes in the material following heat–treatments. In the case of the titanium electrode, the most common failure in the structure was the peeling of the metal layer from the substrate, especially noticeable in the case of 450 ºC heat treatment (Figure 25), which partly destroyed the memristive layer. The formation of the bubbles was assumed to be caused by the thermal expansion coefficient mismatch of the materials. In the case of a copper–coated bottom electrode, diffusion of the electrode material through the memristive layer caused most of the structural failures as shown by the increasing darker areas (Figure 26). The diffused material could also be observed with an optical microscope attached to the probing station used in the electrical measurements. These areas were short circuited with the bottom electrode.
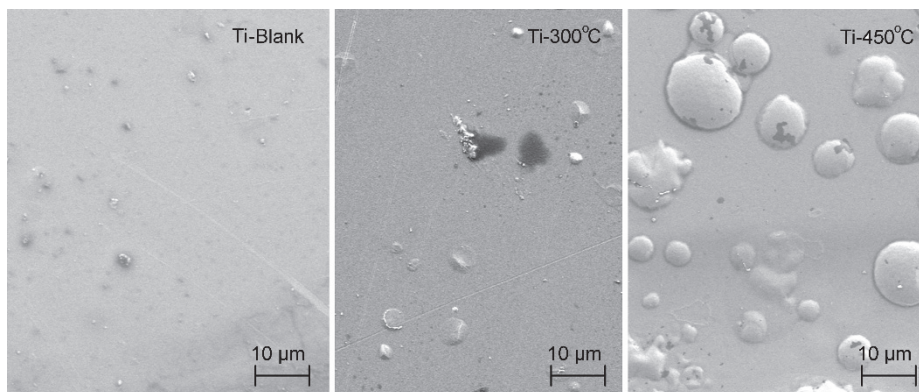
Fig. 25. Secondary emission FESEM pictures of memristors printed on titanium substrate with different heat treatments. Bubbles caused by peeling of the bottom electrode started to appear at temperatures above 300 ˚C, dominating the surface at 450 ˚C. Copyright (c) 2013 The Japan Society of Applied Physics [Paper V].
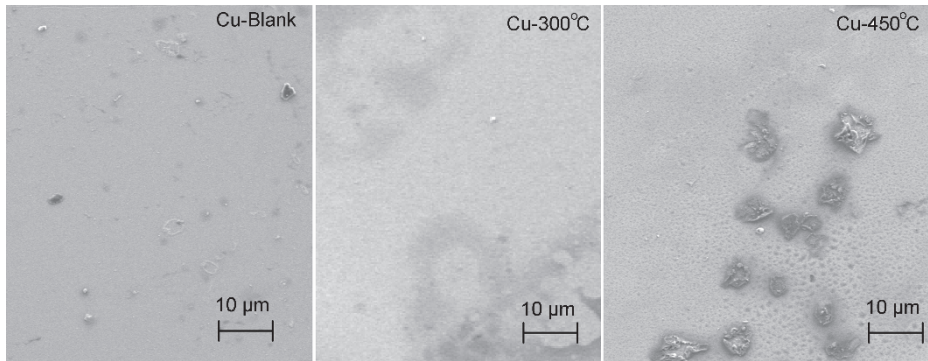
Fig. 26. Secondary emission FESEM pictures of memristors printed on copper substrate with different heat treatments. Diffusion of the bottom electrode material through the memristive layer can be seen as increasing darker areas. Diffused material breaks most of the surface at 450 ˚C. Copyright (c) 2013 The Japan Society of Applied Physics [Paper V].

4.4.3 Adhesion experiments

The printed layers reported in Paper III and Paper IV were tested by two different means in order to obtain data on their adhesion properties. Equipment for the adhesion tests was purchased in 2012 and thus these experiments for the printed layers in Paper I and Paper II were not performed according to the standards. However, it was noted during the printing experiments in Paper II that the adhesion of the printed layers on the copper surfaces of antennas was very good and abrasive methods were needed to remove them.

All printed Co/PMMA patterns printed on PC in Paper III had excellent adhesion in the tape peel tests (5B on the ASTM standard, indicating no peeling of the cured ink). Figure 27 shows a typical cross–hatch cut pattern for a 50 vol.% sample after peeling of the tape. No chips of the cured ink peeled off with the tape from the squares formed during the cutting tests.
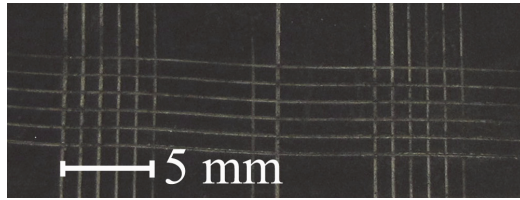
Fig. 27. Example of tape peel test result on cured ink sample containing 50 vol.% of cobalt on PC substrate. No cured ink was peeled from the cut squares. Copyright 2015 by The Minerals, Metals & Materials Society. [Paper III].

The strength values achieved in the pull–off tests for the printed patterns in Paper III were good up to a solids content of 50 vol.%. However, the strength declined with higher loading levels (Figure 28). Resulting pull–off strength values were high compared to those reported earlier for inkjet printed silver inks [87, 88]. For conductive adhesives, somewhat higher shear strength values of 5–6.75 MPa were reported by Cui *et al.* [89]. These values are higher than our results, which is understandable for adhesives. A possible reason for the decreasing adhesion of the cured inks containing 60 and 70 vol.% of cobalt was the increased agglomeration which also increased the porosity, as noted in the FESEM analysis. Consequently the contact area between the binder phase and surface of the substrate was reduced.
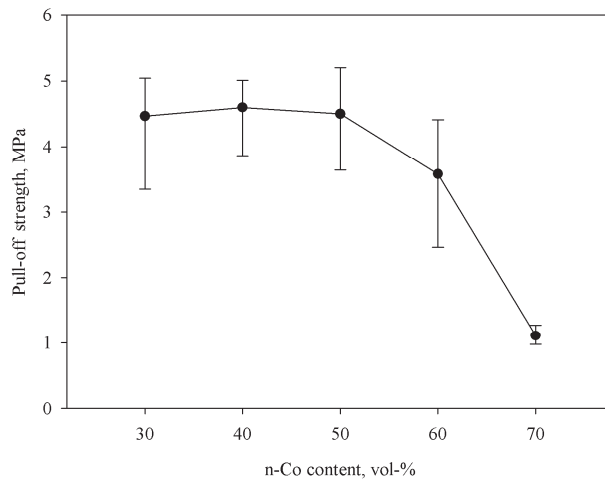
Fig. 28. Pull–off measurement results from three samples of each cured cobalt ink layer indicating moderately high strength of the printed layers on PC up to the cobalt content of 50 vol.%. Copyright 2015 by The Minerals, Metals & Materials Society. [Paper III].

All PZT/P(VDF–TrFE) layers printed on alumina with a silver bottom electrode (DuPont 5064H) in Paper IV achieved the 5B result on the ASTM standard tape peel –tests carried out for the cured piezoelectric inks. Figure 29 shows a typical cross–hatch cut pattern after the tape peel test for the sample with 40 vol.% of PZT. No chips of dried ink were removed with the tape from the squares formed during the cutting tests.
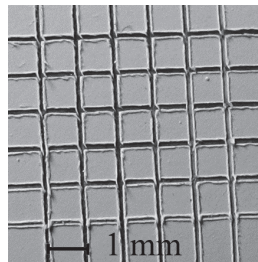
Fig. 29. Typical printed surface after ASTM D–3359–B cross–hatch test. The ink sample contained 40 vol.% of PZT, printed on silver electrode on alumina substrate. No peeling of the ink from the cut pattern could be observed. Copyright 2015 Elsevier. [Paper IV].

The pull–off strengths of the piezoelectric ink samples also indicated that, from the adhesion point of view, the optimal solids content was 40 – 50 vol.%. Figure 30 shows the measured pull–off strength values reaching a maximum of 3.25 MPa at 50 vol.% and then decreasing rapidly. The adhesion still remained relatively high with even higher ceramic loading levels when compared to that of the magnetic inks.
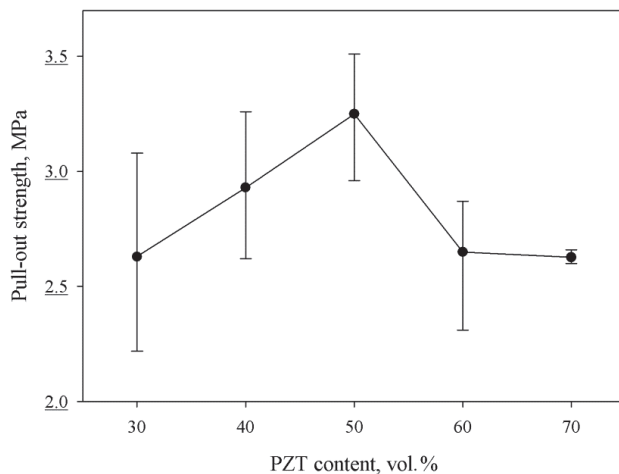
Fig. 30. The results of the pull–off strength tests for the cured piezoelectric inks printed on silver electrode on alumina. Three samples per measurement. A clear decrease of the adhesion was noted at 60 and 70 vol.% loading levels. Copyright 2015 Elsevier. [Paper IV].

4.4.4 Electrical properties of cured patterns of magnetic and piezoelectric inks

The electrical measurements of cured piezoelectric and magnetic inks are presented in Papers I–IV in more detail than in this thesis because they were the contributions of the co–authors. Errata of the electrical measurements [90, 91] for Papers I and II describe the electrical properties of cured inks as being similar to those in Paper III. The errata was done due to error on magnetic properties calculations on Papers I and II. In Paper III, relative permeability values up to 3 and loss tangents up to 0.01 at 2 GHz were achieved. The permeability of the layers increased in proportion to the content of Co at 30–50 vol.%. With higher Co content (60 vol.%) the permeability started to decrease, which can be explained by the increase in porosity observed in the FESEM analysis.

In Paper IV the cured piezoelectric ink layers achieved the maximum permittivity value of 48 at 1 kHz frequency with a loading level of 50 vol.% of PZT, after which the permittivity decreased. In this case the main explanation is also the increased porosity. The piezoelectric constant d_{31} increased to the value of 17 pm/V

61

when the amount of PZT increased to 50 vol.%. Polarization of the samples with higher PZT content was not possible due to the electrical breakdowns.

4.4.5 Electrical properties of memristors

Electrical measurements carried out on the precursor samples printed on titanium or copper showed memristive properties. Without additional heat–treatments the resistance values and degree of shifting were similar with both electrode materials. Generally the printed memristors utilizing the titanium layer endured more read/erase –cycles (up to 30) than those with the copper electrodes (up to 15 cycles) before breakage. Typical voltage/resistance and voltage/current –cycles for the printed structures with titanium and with copper electrodes are shown in Figures 31 and 32.
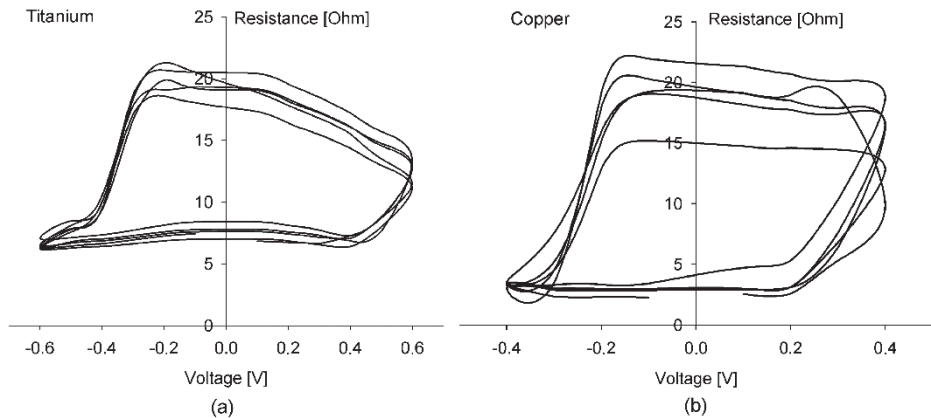
Fig. 31. Voltage/resistance cycles for the printed memristive structures with (a) titanium and (b) copper electrodes, without additional heat–treatment. Copyright (c) 2013 The Japan Society of Applied Physics. [Paper V].
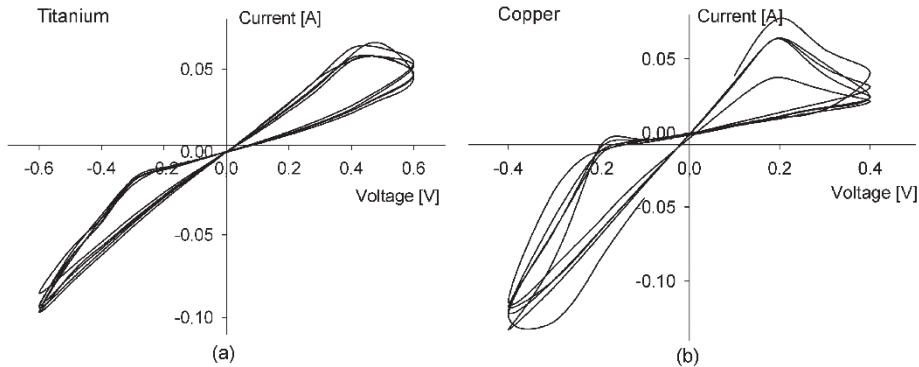
Fig. 32. Current/voltage curves for the printed memristive structures with (a) titanium and (b) copper electrodes, without additional heat–treatment Copyright (c) 2013 The Japan Society of Applied Physics. [Paper V].

The typical low resistance state of the printed structures with titanium electrodes had a higher resistance than those with copper, whereas the high resistance states were similar. Moreover, the shifting occurred at –0.4 and 0.5 V with a titanium electrode and at –0.3 V and 0.3V with copper. The related resistance values of 8 and 20 Ω and 3 and 20 Ω were obtained, respectively. The structures using titanium electrodes exhibited a more stable shifting of the resistance values compared to those on copper. The latter had a tendency to degrade the resistance values progressively during the read/erase –cycles, finally leading to a short–circuiting of the sample. Thus, the use of a titanium electrode contributed a stabilizing effect on the resistance properties of memristors, as also reported by Yang *et al.* [63]. In addition, the higher values in the lower resistance state, typical for the structures with titanium electrodes, are beneficial for the durability of memristors since the current passing through the component is reduced.

In heat–treatment experiments it was noted that the resistance shifting of the samples with titanium electrodes increased by up to 3 orders of magnitude. The resistance shifting in the case of copper electrodes was minimal. This is probably due to interactions between the memristive precursor layer and the bottom electrode. The treatments carried out at temperatures higher than 350 ºC greatly reduced the number of areas with memristive functionality, presumably due to the structural failures discussed in the results of the FESEM analysis. The results of voltage/resistance measurements carried out on the samples treated at 300 ºC are shown on Figure 33. The shifting voltages of a printed memristor with a titanium electrode changed from –0.4 and 0.5 V for the untreated sample to –0.3 and 0.2 V.

The low resistance state increased from $10 - 50$ Ω in the original sample to 30–100 Ω after the heat–treatment, whereas the high resistance state increased from 20–250 Ω to 5–12 kΩ, respectively.
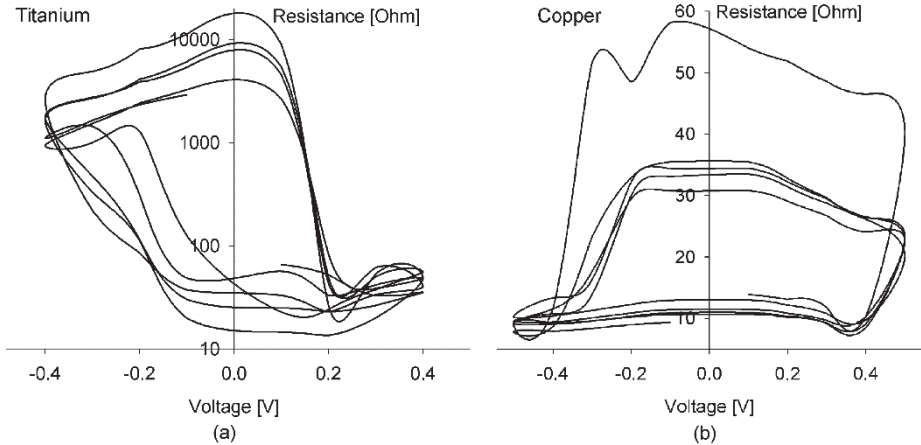
Fig. 33. Voltage/resistance curves of memristors treated at 300 ºC with (a) titanium and (b) copper electrodes. The resistance scale in (a) is logarithmic due to the large shifting of the resistance. Copyright (c) 2013 The Japan Society of Applied Physics. [Paper V].

The disadvantage of the heat–treatment of the memristor samples was the fluctuation of the resistance values and the reduced durability. After the heat–treatment the best memristors with titanium electrodes endured only five read/erase –cycles. For the memristors with copper electrodes, the heat–treatments did not have any remarkable influence on the resistance values or shifting voltages, indicating that the chemical interaction of copper with the memristive precursor was neglible. Also, the measured fluctuation in the resistance values remained similar to that of the samples without heat–treatments. However, the quantity of memristive areas was reduced greatly following the heat–treatments, which was expected from the FESEM analysis.

The measured average resistance values of the heat–treated samples are collected on Table 3. Measurement results for samples surviving more than three read/erase –cycles were collected and the average values were calculated. The heat–treatments had a positive influence on the resistance shifting in the samples with titanium electrodes. As the temperature increased above 350 ºC, the reliability of the performance of the samples decreased. This can be seen from the number of

cycles that could be measured from the samples on different areas i.e. the more memristive areas that could be found, the greater the number of cycles that could be measured. In the case of copper electrodes, a significant increase in resistance values was not observed and there were fewer functional areas than in the samples printed on titanium.

Table 3. Development of resistance values as a function of heat–treatments. Average resistance values were obtained from the samples enduring three or more read/erase –cycles. The number of measured cycles reflects the durability of the samples. Higher heat–treatment temperatures decreased the number of functional areas and the endurance of read/erase –cycles. [Paper V].

Titanium substrate					Copper substrate				
Treatment t / °C	Lower resistance [Ohm]	Higher resistance [Ohm]	Number of cycles	Number of functional samples	Treatment t / °C	Lower resistance [Ohm]	Higher resistance [Ohm]	Number of cycles	Number of functional samples
Blank	40	200	45	10	Blank	6	16	14	4
250	30	140	37	7	250	4	20	6	2
300	80	2300	32	7	300	13	35	13	4
350	250	5600	19	6	350	12	38	18	5
400	50	14500	15	5	400	-	-	0	0
450	20000	100000	6	2	450	35	550	7	2

5   Conclusions

A novel method for producing magnetic nanoparticle ink from dry Co powder for high frequency applications was developed In Paper I. The printed ink layers were demonstrated to yield relatively high magnetic permeability films at high frequencies. The formulated inks could be cured at low temperatures that are compatible with various organic substrates. The most suitable cobalt content in the ink for screen printing was 60 wt.% (14 vol.%) and demonstrated the best defined linewidths, the best uniformity of the printed patterns and the most homogenous distribution of the particles in the printed layers.

The utilization of unsaturated fatty acid both as a surfactant and binder with Co nanoparticles in printed electronics applications was developed in Paper II. The solids contents were greatly increased compared to those of Paper I, reaching 88 wt.% (50 vol.%) of Co. The adhesion of the ink to the metallic surfaces on the antennas was good due to the covalent bonding between the copper surface and the carboxylic acid groups of the linoleic acid. Furthermore, no sedimentation of the particles in the ink was observed in the cross–section studies of the printed patterns. Also, the ink remained printable after one year of storage in a sealed container at room temperature. The feasibility of the developed ink has also been shown for dual–band monopole antennas [72].

Magnetic inks with excellent adhesion characteristics on PC substrates were developed In Paper III. The quality of the printed structures was sufficient for inks with 30–50 vol.% (77–88 wt.%) of Co. The best adhesion and electromagnetic properties were achieved after printing one layer of the ink containing 50 vol.% of Co. The achieved pull–off strength was higher than that reported earlier for inkjet printed conductive inks, being comparable with conductive adhesives.

Low curing temperature piezoelectric composite inks were developed in Paper IV using commercially available PZT and P(VDF–TrFE) copolymer powders. The ceramic loading in the composite was varied between 30–70 vol.% (64–91 wt.%). The samples were successfully printed on a silver bottom electrode on a substrate of PET film or alumina. The inks with up to 50 vol.% (81 wt.%) ceramic particles showed uniform microstructures and good adhesion in the pull–off and cross–hatch tape–peel tests.

Inkjet printable memristive ink was developed in Paper V. A novel synthesis route for the titanium oxide precursor was developed and the resulting solution was further formulated into inkjet printable form. The solution was printed both on titanium and copper electrodes, achieving memristive properties on both materials.

The most suitable thickness for the memristive layer of the synthesised precursor material was determined to be 70–80 nm. The use of a titanium layer as the bottom electrode increased the lifetime and shifting of the resistance value of the memristors. This was especially the case when the heat–treatment at 300 °C was used, where a resistance change of 3 orders of magnitude was obtained. The use of titanium electrodes also increased the endurance of the memristors in write/erase – cycles up to 30 cycles while the copper electrodes withstood up to only 15 cycles. In addition, the precursor material synthesised was observed to remain functional even after one year of storage.

In general, the research results show that printed electronics offer an interesting alternative for traditional manufacturing methods of electronics. It was also observed that current printed electronics production processes can be even more simplified by utilizing dry powders as raw materials instead of synthesizing the desired particles in order to form inks. Moreover, this approach offers a very wide selection of raw materials with a reasonable price and large quantities, thus opening further opportunities for novel printed electronics products. By careful selection of feasible surfactant both ink formulation and its process flow can be simplified without sacrificing the printability and the quality of the cured layer.

In the case of piezoelectric inks, the work carried out in selecting correct matrix material enabled the development of printable composite ink where both the filler and matrix polymer were piezoelectric.

The memristors research provided totally new approach to develop a functional ink based on synthesized organometallic precursor obtaining characteristics that could be utilized as printable non–volatile memories. The structures commonly fabricated by the thin film process could be now realized with a laboratory tabletop inkjet printer.

All the inks developed obtained relatively good adhesion on the used polymer or metal substrate, indicating that the binders used for the inks were successfully selected. Naturally further studies are needed, if the electrical values such as permeability or piezoelectric coefficients need to be optimized for specific applications. In the case of piezoelectric inks also the shelf life of the product should be further developed by for example utilizing surfactants. If the inks are aimed to be utilized in larger scale practical applications, more work is also needed for upscaling the ink manufacturing processes and determining the needed parameters to keep the production batches constant in quality.

The magnetic inks developed in this work may be used in future applications such as printed antennas, especially for their miniaturization when fabricated on

plastic substrates, as demonstrated in Paper II and [72]. The use of an oxidative polymerizing fatty acid as a surfactant and binder will almost certainly have future use in printed electronics when the use of copper or aluminium based inks increases on printed conductive patterns, due to its bonding capability especially with those metals. The piezoelectric inks have a clear application field especially in printed sensors to be used for example in wearable electronics. Memristors provide an interesting option to add memory to small printed goods such as smart cards. With the help of novel products and innovations, the cost–effective and simple manufacturing methods of printed electronics will bring the ubiquitous electronics world even closer to our everyday life.

References

1. Berggren M, Nilsson D & Robinson ND (2007) Organic materials for printed electronics. Nature Materials 6(1): 3–5.
2. Kang B, Lee WH & Cho K (2013) Recent advances in organic transistor printing processes. ACS Applied Materials and Interfaces 5(7): 2302–2315.
3. Kim SH, Hong K, Xie W, Lee KH, Zhang S, Lodge TP & Frisbie CD (2013) Electrolyte–gated transistors for organic and printed electronics. Advanced Materials 25(13): 1822–1846.
4. Voigt JFH & Haeffner JA (1899) Electrical Resistance. US patent 617375A.
5. Deyrup AJ, Kermit H, Ballard K & Strickarz JJ (1945) Preparation of electrical capacitors. US patent 2389419.
6. Hoffman LC (1984) An overwiev of thick–film hybrid materials. American Ceramic Bulletin 63: 572–576.
7. Prudenziati M & Hormadaly J (2012) Printed Films: Materials Science and Applications in Sensors, Electronics and Photonics. Woodhead Publishing Limited: 5–6.
8. Kirby PL (1989) Origins and advances in polymer thick–film technology. Proceedings of 7th European Hybrid Microelectronics Conference, Hamburg: Paper 4.1.
9. Gilleo K (1996) Polymer Thick Film: Today's Emerging Technology for a Clean Environment Tomorrow. Springer Science & Business Media.
10. Tseng C–C, Chang C–P, Sung Y, Chen Y–C & Ge M–D (2009) A novel method to produce Pd nanoparticle ink for ink–jet printing technology. Colloids and Surfaces A: Physicochemical and Engineering Aspects 339(1–3): 206–210.
11. Teja AS & Koh P–Y (2009) Synthesis, properties, and applications of magnetic iron oxide nanoparticles. Progress in Crystal Growth and characterization of Materials 55(1–2): 22–45.
12. K. Hagen (2008) Organic Electronics. Weinheim: WILEY–VCH Verlag.
13. Brabec C, Scherf U & Dyakonov V (2011) Organic Photovoltaics: Materials, Device Physics, and Manufacturing Technologies. John Wiley & Sons.
14. Kipphan H (2001) Handbook of print media. Heidelberg, Germany: Springer–Verlag: 55–70.
15. Stephens J (2000) Screen printing in a digital age. Pira International.
16. Pekarovicova A & Pekarovic J (2001) Flexo printability of publication grades: technical challenges of publication flexography. 53rd Annual technical conference of TAGA, San Diego.
17. Savastano D (2005) The flexo ink market. Ink World 83.
18. Perelaer J, Smith PJ, Mager D, Soltman D, Volkman SK, Subramanian V, Korvink JG & Schubert US (2010) Printed electronics: the challenges involved in printing devices, interconnects, and contacts based on inorganic materials. Journal of Material Chemistry 20: 8446–8453.

19. Hong CM, Gleskova H & Wagner S (1997) Direct Writing and Lift–Off Patterning of Copper Lines at 200°C Maximum Process Temperature. Materials Research Society Symposium Proceedings 471.

20. Redinger DR, Molesa S, Yin S, Farschi R, Subramanian V (2004) An Ink–Jet–Deposited Passive Component Process for RFID. IEEE Transactions on Electron Devices 51(12).

21. O'Connell CD, Higgins MJ, Sullivan RP, Jamali SS, Moulton SE & Wallace GG (2013) "Nanoscale platinum printing on insulating substrates". Nanotechnology 24(50): 505301–505311.

22. Fei F, Zhuang J, Wu W, Song M, Zhang D, Li S, Su W & Cui Z (2015) A printed aluminum cathode with low sintering temperature for organic light–emitting diodes. RSC Advances 5: 608–611.

23. Solanki JN & Murthy ZVP (2011) Controlled Size Silver Nanoparticles Synthesis with Water–in–Oil Microemulsion Method: A Topical Review. Industrial & Engineering Chemistry Research 50: 12311–12323.

24. Chaikin Y, Bendikov TA, Cohen H, Vaskevich A & Rubinstein I (2013) Phosphonate–stabilized silver nanoparticles: One–step synthesis and monolayer assembly. Journal of Materials Chemistry C 1(22): 3573–3583.

25. Perelaer J, Hendriks CE de Laat AWM & Schubert US (2009) One–step inkjet printing of conductive silver tracks on polymer substrates. Nanotechnology 20: 165303.

26. Siponkoski T, Nelo M, Peräntie J, Juuti J & Jantunen H (2015) BaTiO3–P(VDF–TrFE) composite ink properties for printed decoupling capacitors. Composites Part B: Engineering 70: 201–205.

27. Allen M, Aronniemi M, Mattila T, Helistö P, Sipola H, Rautiainen A, Leppäniemi J, Alastalo A, Korhonen R & Seppä H (2011) Contactless read–out of printed memory. Microelectronic Engineering 88(9): 2941–2945.

28. Rendl C, Greindl P, Haller M, Zirkl M, Stadlober B & Hartmann P (2012) PyzoFlex: Printed piezoelectric pressure sensing foil. UIST'12 – Proceedings of the 25th Annual ACM Symposium on User Interface Software and Technology: 509–518.

29. Yang T, Brown RNC, Kempel LC & Kofinas P (2010) Surfactant–modified nickel zinc iron oxide/polymer nanocomposites for radio frequency applications. Journal of Nanoparticle Research 12(8): 2967–2978.

30. Moser A, Takano K, Margulies DT, Albrecht M, Sonobe Y, Ikeda Y, Sun S & Fullerton EE (2002) Magnetic recording: Advancing into the future. Journal of Physics D 35(19): R157–R167.

31. Bigioni TP, Lin X, Nguyen TT, Corwin EI, Witten TA & Jaeger HM (2006) Kinetically driven self–assembly of highly ordered nanoparticle monolayers. Nature Materials 5(4): 265–270.

32. Rudenkiy S, Frerichs M, Voigts F, Maus–Friedrichs W, Kempter V, Brinkmann R, Matoussevitch N, Brijoux W, Bönnemann H, Palina N & Modrow H (2004) Study of the structure and stability of cobalt nanoparticles for ferrofluidic applications. Applied Organometallic Chemistry 18(10): 553–560.

33. Mornet S, Vasseur S, Grasset F & Duguet E (2004) Magnetic nanoparticle design for medical diagnosis and therapy. Journal of Materials Chemistry 14(14): 2161–2175.

34. Neuberger T, Schöpf B, Hofmann H, Hofmann M & Von Rechenberg B (2005) Superparamagnetic nanoparticles for biomedical applications: Possibilities and limitations of a new drug delivery system. Journal of Magnetism and Magnetic Materials 293(1): 483–496.

35. Hu A, Yee GT & Lin W (2005) Magnetically recoverable chiral catalysts immobilized on magnetite nanoparticles for asymmetric hydrogenation of aromatic ketones. Journal of the American Chemical Society 127(36): 12486–12487.

36. Pohjalainen E, Pohjakallio M, Johans C, Kontturi K, Timonen JVI, Ikkala O, Ras RHA, Viitala T, Heino MT & Seppälä ET (2010) Cobalt nanoparticle langmuir–schaefer films on ethylene glycol subphase. Langmuir 26(17): 13937–13943.

37. Aleksandrovic V, Greshnykh D, Randjelovic I, Frömsdorf A, Kornowski A, Roth SV, Klinke C & Weller H (2008) Preparation and electrical properties of cobalt – platinum nanoparticle monolayers deposited by the langmuir – blodgett technique. ACS Nano 2(6): 1123–1130.

38. Ago H, Qi J, Tsukagoshi K, Murata K, Ohshima S, Aoyagi Y & Yumura M (2003) Catalytic growth of carbon nanotubes and their patterning based on ink–jet and lithographic techniques. Journal of Electroanalytical Chemistry 559: 25–30.

39. Safari A & Akdogan EK (2008) Piezoelectric and Acoustic materials for Transducer Applications. Springer.

40. Moulson AJ (1971) Electroceramics, 2nd Edition. Chapman and Hall.

41. Subramanian V, Chang JB, Vornbrock AF, Huang DC, Jagannathan L, Liao F, Mattis B, Molesa S, Redinger DR, Soltman D, Volkman SK & Qintao Z (2008) Printed Electronics For Low–Cost Electronic Systems: Technology Status and Application Development. ESSDERC 2008 – Proceedings of the 38th European Solid–State Device Research Conference, art. no. 4681785: 17–24.

42. Parashkov R, Becker E, Riedl T, Johannes H–H & Kowals W (2005) Large Area Electronics Using Printing Methods. Proceedings of the IEEE 93: 1321–1329.

43. Virtanen J, Ukkonen L, Björninen T, Elsherbeni, AZ, Sydänheimo L (2011) Inkjet–Printed Humidity Sensor for Passive UHF RFID Systems. IEEE Transactions on Instrumentation and Measurement, 60, art. no. 5759086: 2768–2777.

44. Hübler AC, Bellmann M, Schmidt GC, Zimmermann S, Gerlach A & Haentjes C (2012) Fully mass printed loudspeakers on paper. Organic Electronics: physics, materials, applications 13: 2290–2295.

45. Tajitsu Y & Chiba A (1980) Crystalline phase transition in the copolymer of vinylidenefluoride and trifluoroethylene. Applied Physics Letters 36: 286–288.

46. Koga K & Ohigashi H (1986) Piezoelectricity and related properties of vinylidene fluoride and trifluoroethylene copolymers. Journal of Applied Physics 59: 2142–2150.

47. Cheng Z–Y, Bharti V, Xu T–B, Xu H, Mai T & Zhang Q.M (2001) Electrostrictive poly(vinylidene fluoride–trifluoroethylene) copolymers. Sensors and Actuators, A: Physical 90(1-2): 138–147.

48. Chen Q, Natale D, Neese B, Ren K, Lin M & Zhang QM (2007) Piezoelectric Polymers Actuators for Precise Shape Control of Large Scale Space Antennas. Proceedings of SPIE – The International Society for Optical Engineering art. no. 65241P.

49. Zhang D–Q, Wang D–W, Yuan J, Zhao Q–L, Wang Z–Y & Cao M–S (2008) Structural and Electrical Properties of PZT/PVDF Piezoelectric Nanocomposites Prepared by Cold–Press and Hot–Press Routes. Chinese Physics Letters 25: 4410–4413.

50. Hu Z, Tian M, Nysten B & Jonas AM (2009) Regular arrays of highly ordered ferroelectric polymer nanostructures for non–volatile low–voltage memories. Nature Materials 8: 62–67.

51. Tomer V, Manias E & Randall CA (2011) High field properties and energy storage in nanocomposite dielectrics of poly(vinylidene fluoride–hexafluoropropylene). Journal of Applied Physics 110: art. no. 044107.

52. Canavese G, Stassi S, Cauda V, Verna A, Motto P, Chiodoni A, Marasso SL & Demarchi D (2013) Different Scale Confinements of PVDF–TrFE as Functional Material of Piezoelectric Devices. IEEE Sensors Journal 13(6): 2237–2244.

53. Chua LO (1971) Memristor – the missing circuit element. IEEE Transactions on Circuit Theory CT–18: 507–519.

54. Chua LO & Kang SM (1976) Memristive devices and systems. Proceedings of the IEEE 64: 209–223.

55. Argall F (1968) Switching phenomena in titanium oxide thin films. Solid–State Electronics 11: 535–541.

56. Strukov DB, Snider GS, Stewart DR & Williams RS (2008) The missing memristor found. Nature 453: 80–83.

57. Yang JJ, Pickett MD, Li X, Ohlberg DAA, Stewart DR & Williams RS (2008) Memristive switching mechanism for metal/oxide/metal nanodevices. Nature Nanotechnology 3: 429.

58. Kwon D–H, Kim KM, Jang JH, Jeon JM, Lee MH, Kim GH, Li X–S, Park G–S, Lee B, Han S, Kim M & Hwang CS (2010) Atomic structure of conducting nanofilaments in TiO_2 resistive switching memory. Nature Nanotechnology 5: 148–153.

59. Xia Q, Robinet W, Cumbie MW, Banerjee N, Cardinali TJ, Yang JJ, Wu W, Li X, Tong WM, Strukov DB, Snider GS, Medeiros–Ribeiro G & Williams RS (2009) Memristor−CMOS Hybrid Integrated Circuits for Reconfigurable Logic. Nano Letters 9: 3640.

60. Jo SH., Kim K–H, and Lu W (2009) High–Density Crossbar Arrays Based on a Si Memristive System. Nano Letters 9(2).

61. Borghetti J, Snider GS, Kuekes PJ, Yang JJ, Stewart DR & Williams RS (2010) Memristive' switches enable 'stateful' logic operations via material implication. Nature 464.

62. Xia Q (2011) Nanoscale resistive switches: devices, fabrication and integration. Applied Physics A 102: 955–965.

63. Yang JJ, Strachan JP, Miao F, Zhang M–X, Pickett MD, Yi W, Ohlberg DAA, Ribeiro GM & Williams RS (2011) Metal/TiO_2 interfaces for memristive switches. Applied Physics A 102: 785–789.

64. Lian K, Li R, Wang H, Zhang J & Gamota D (2010) Printed flexible memory devices using copper phthalocyanine. Materials Science and Engineering B 167: 12–16.
65. Gergel–Hackett N, Hamadani B, Dunlap B, Suehle J, Richter C, Hacker C & Gundlach D (2009) A Flexible Solution–Processed Memristor. IEEE Electron Device Letters 30: 706–708.
66. Ng TN, Russo B & Arias AC (2011) Solution–Processed Memristive Junctions Used in a Threshold Indicator. IEEE Transactions on Electron Devices 58: 3435.
67. Shih A, Zhou W, Qiu J, Yang H–J, Chen S, Mi Z & Shih I (2010) Highly stable resistive switching on monocrystalline ZnO. Nanotechnology 21.
68. Tanaka Y & Suganuma M (2001) Effects of Heat Treatment on Photocatalytic Property of Sol–Gel Derived Polycrystalline TiO2. Journal of Sol–Gel Science and Technology 22: 83–89.
69. Xanthos, M (2010) Functional fillers for plastics 2nd. ed. Viley–Verlag: 112–119.
70. Ghasemi E, Mirhabibi A & Edrissi M. (2008) Synthesis and rheological properties of an iron oxide ferrofluid. Journal of Magnetism and Magnetic Materials 320: 2635–2639.
71. García–Jimenoa S & Estelrich J (2013) Ferrofluid based on polyethylene glycol–coated iron oxide nanoparticles. Colloids and Surfaces A: Physicochemical and Engineering Aspects 420: 74–81.
72. Sowpati AK, Nelo M, Palukuru VK, Juuti J & Jantunen H (2013) Miniaturisation of dual band monopole antennas loaded with screen printed cobalt nanoparticle ink. IEEE Microwaves, Antennas and Propagation 7(3): 180–186.
73. Rao CRK & Trivedi DC (2006) Biphasic synthesis of fatty acids stabilized silver nanoparticles: Role of experimental conditions on particle size. Materials Chemistry and Physic 99: 354–360.
74. Bell NS, Schendel ME & Piech M (2005) Rheological properties of nanopowder alumina coated with adsorbed fatty acids. Journal of Colloid and Interface Science 287: 94–106.
75. Lan Q, Liu C, Yang F, Liu S, Xu J & Sun D (2007) Synthesis of bilayer oleic acid–coated Fe3O4 nanoparticles and their application in pH–responsive pickering emulsions. Journal of Colloid and Interface Science 310: 260–269.
76. Sailer RA & Soucek MD (2000) Investigation of cobalt drier retardation. European Polymer Journal 36: 803–811.
77. Van den Berg JDJ (2002) Analytical chemical studies on Traditional Linseed Oil Paints. Doctoral thesis. Universiteit van Amsterdam: 18–40.
78. Chan HW–S (1987) Autoxidation of unsaturated lipids. Food and Science technology. Academic press, London: 1–16.
79. Mallègol J, Gononm L & Commereuc S (2001) Thermal (DSC) and Chemical (Iodometric Titration) Methods for Peroxides Measurements on Order to Monitor Drying Extent of Alkyd Resins. Progress on Organic coatings 41: 171–176.
80. Janeczeka K, Kozioła G, Jakubowska M, Arazna A, Młozniak A, & Futera, K. (2013) Assessment of electromechanical properties of screen printed polymer nanopastes. Materials Science and Engineering B 178: 511–519.

81. Jakubowska M, Sloma M & Młozniak A (2011) Printed transparent electrodes containing carbon nanotubes for elastic circuits applications with enhanced electrical durability under severe conditions. Materials Science and Engineering B 176: 358–362.

82. Kim JY, Kim SH, Lee H–H, Lee K, Ma W, Gong X & Heeger AJ (2006) New Architecture for High–Efficiency Polymer Photovoltaic Cells Using Solution–Based Titanium Oxide as an Optical Spacer. Advanced Materials 18: 572–576.

83. Phillips NJ & Milne SJ (1991) Diol–based Sol–Gel System for the Production of Thin Films of $PbTiO_3$. Journal of Materials Chemistry 5: 893–894.

84. Dang Z–M, Shen Y & Nan C–W (2002) Dielectric behavior of three–phase percolative Ni–$BaTiO_3$/polyvinylidene fluoride composites. Applied Physics Letters 81: 4814–4816.

85. Ploss B, Ng W–Y, Chan HL–W & Choy C–L (2001) Poling study of PZT/P(VDF–TrFE) composites. Composites Science and Technology 61: 957–962.

86. Yang W, Yu S, Sun R & Du R (2011) Nano– and microsize effect of CCTO fillers on the dielectric behavior of CCTO/PVDF composites. Acta Materialia 59: 5593–5602.

87. Sridhar A, van Dijk DJ & Akkerman R (2009) Inkjet printing and adhesion characterisation of conductive tracks on a commercial printed circuit board material. Thin Solid Films 517: 4633–4637.

88. Caglar U, Kaija K & Mansikkamaki P (2009) Evaluation of adhesion pull–off performance of nanoparticle–based inkjet–printed silver structure on various substrates. International Journal of Nanotechnology 6: 681–690.

89. Cui H–W, Jiu J–T, Nagao S, Sugahara T, Suganuma K, Uchida H & Schroder KA (2014) Ultra–fast photonic curing of electrically conductive adhesives fabricated from vinyl ester resin and silver micro–flakes for printed electronics. RSC Advances (4): 15914.

90. Nelo M, Sowpati A, Palukuru VK, Juuti J & Jantunen H. (2014) Errata to Formulation of screen printable cobalt nanoparticle ink for high frequency applications. Progress in Electromagnetic Research Letters 50: 99–100.

91. Nelo M, Sowpati A, Palukuru VK, Juuti J & Jantunen, H (2014) Errata to Utilization of screen printed low curing temperature cobalt nanoparticle ink for miniaturization of patch antennas. Progress in Electromagnetic Research Letters 50: 101–102.

Original papers

I   Nelo M, Sowpati AK, Palukuru VK, Juuti J & Jantunen H (2010) Formulation of screen printable cobalt nanoparticle ink for high frequency applications. Progress In Electromagnetics Research 110: 253–266

II   Nelo M, Sowpati AK, Palukuru VK, Juuti J & Jantunen H (2012) Utilization of screen printed low curing temperature cobalt nanoparticle ink for miniaturization of patch antennas. Progress In Electromagnetics Research 127: 427–444

III Nelo M, Myllymäki S, Juuti J, Uusimäki A & Jantunen H (2015) Cobalt nanoparticle inks for printed high frequency applications on polycarbonate. Journal of Electronic Materials 44(12): 4884–4890.

IV Siponkoski T, Nelo M, Palosaari J, Peräntie J, Sobocinski M, Juuti J & Jantunen H (2015) Electromechanical properties of PZT/P(VDF–TrFE) composite ink printed on a flexible organic substrate. Composites Part B: Engineering 80: 217–222.

V   Nelo M, Sloma M, Kelloniemi J, Puustinen J, Saikkonen T, Juuti J, Häkkinen J, Jakubowska M & Jantunen H (2013) Inkjet–printed memristor – printing process development. Japanese Journal of Applied Physics 52(5): article 05DB21.

Published papers have been reprinted with premission from The Electromagnetics Academy (I-II), The Minerals, Metals & Materials Society (III), Elsevier Limited (IV) and The Japan Society of Applied Physics (V).

Original publications are not included in the electronic version of the dissertation

537. Komulainen, Jukka (2015) Software-based countermeasures to 2D facial spoofing attacks

538. Pedone, Matteo (2015) Algebraic methods for constructing blur-invariant operators and their applications

539. Karhu, Mirjam (2015) Treatment and characterisation of oily wastewaters

540. Panula-Perälä, Johanna (2015) Development and application of enzymatic substrate feeding strategies for small-scale microbial cultivations : applied for *Escherichia coli*, *Pichia pastoris*, and *Lactobacillus salivarius* cultivations

541. Pennanen, Harri (2015) Coordinated beamforming in cellular and cognitive radio networks

542. Ferreira, Eija (2015) Model selection in time series machine learning applications

543. Lamminpää, Kaisa (2015) Formic acid catalysed xylose dehydration into furfural

544. Visanko, Miikka (2015) Functionalized nanocelluloses and their use in barrier and membrane thin films

545. Gilman, Ekaterina (2015) Exploring the use of rule-based reasoning in ubiquitous computing applications

546. Kemppainen, Antti (2015) Limiting phenomena related to the use of iron ore pellets in a blast furnace

547. Pääkkönen, Tiina (2015) Improving the energy efficiency of processes : reduction of the crystallization fouling of heat exchangers

548. Ylä-Mella, Jenni (2015) Strengths and challenges in the Finnish waste electrical and electronic equipment recovery system : consumers' perceptions and participation

549. Skön, Jukka-Pekka (2015) Intelligent information processing in building monitoring systems and applications

550. Irannezhad, Masoud (2015) Spatio-temporal climate variability and snow resource changes in Finland

551. Pekkinen, Leena (2015) Information processing view on collaborative risk management practices in project networks

552. Karjalainen, Mikko (2015) Studies on wheat straw pulp fractionation : Fractionation tendency of cells in pressure screening, hydrocyclone fractionation and flotation

ACTA UNIVERSITATIS OULUENSIS

SERIES EDITORS

A
SCIENTIAE RERUM NATURALIUM

Professor Esa Hohtola

B
HUMANIORA

University Lecturer Santeri Palviainen

C
TECHNICA
Postdoctoral research fellow Sanna Taskila

D
MEDICA

Professor Olli Vuolteenaho

E
SCIENTIAE RERUM SOCIALIUM
University Lecturer Veli-Matti Ulvinen

F
SCRIPTA ACADEMICA
Director Sinikka Eskelinen

G
OECONOMICA

Professor Jari Juga

H
ARCHITECTONICA
University Lecturer Anu Soikkeli

EDITOR IN CHIEF

Professor Olli Vuolteenaho

PUBLICATIONS EDITOR

Publications Editor Kirsti Nurkkala

UNIVERSITY of OULU
OULUN YLIOPISTO